coatings

MDPI

Review

Corrosion of Anodized Titanium Alloys

Jesús Manuel Jáquez-Muñoz [1,*], Citlalli Gaona-Tiburcio [2], Ce Tochtli Mendez-Ramirez [3], Martha Guadalupe Carrera-Ramirez [1], Miguel Angel Baltazar-Zamora [3], Griselda Santiago-Hurtado [4], Maria Lara-Banda [2], Francisco Estupiñan-Lopez [2], Demetrio Nieves-Mendoza [3] and Facundo Almeraya-Calderon [2,*]

[1] Instituto de Ingeniería y Tecnología, Universidad Autónoma de Ciudad Juárez, Ciudad Juárez 66455, Mexico; martha.carrera@uacj.mx
[2] Universidad Autónoma de Nuevo León, FIME, Centro de Investigación e Innovación en Ingeniería Aeronáutica (CIIIA), San Nicolás de los Garza 66455, Mexico; citlalli.gaonatbr@uanl.edu.mx (C.G.-T.); maria.laraba@uanl.edu.mx (M.L.-B.); francisco.estupinanlp@uanl.edu.mx (F.E.-L.)
[3] Facultad de Ingeniería Civil, Universidad Veracruzana, Xalapa 91000, Mexico; cmendez@uv.mx (C.T.M.-R.); mbaltazar@uv.mx (M.A.B.-Z.); dnieves@uv.mx (D.N.-M.)
[4] Facultad de Ingeniería Civil, Universidad Autónoma de Coahuila, Torreón 27276, Mexico; santiagog@uadec.edu.mx
* Correspondence: jesus.jaquezmn@uanl.edu.mx (J.M.J.-M.); facundo.almerayacld@uanl.edu.mx (F.A.-C.)

Abstract: Ti and Ti alloys are employed in demanding industries such as aerospace, automotive, biomedical, aeronautic, structural, naval, and chemical, thanks to their resistance to corrosion due to the formation of the TiO_2 film on the surface. Diverse research has established that different corrosive media could attack the oxide layer. One way to generate a stable, compact, and continuous oxide film is through anodizing treatment. The efficiency of anodization depends on diverse factors such as the microstructure, chemical composition of alloys, pH of electrolyte, time, and temperature of anodizing. This review aims to examine the corrosion resistance of the anodized layer on Ti and Ti alloys, with different parameters. The discussion is centered on the influence of the different parameters and alloy properties in the effectivity of anodizing when they are characterized by electrochemical techniques while studying the behavior of oxide.

Keywords: titanium; anodizing; electrochemical techniques; corrosion

Citation: Jáquez-Muñoz, J.M.; Gaona-Tiburcio, C.; Mendez-Ramirez, C.T.; Carrera-Ramirez, M.G.; Baltazar-Zamora, M.A.; Santiago-Hurtado, G.; Lara-Banda, M.; Estupiñan-Lopez, F.; Nieves-Mendoza, D.; Almeraya-Calderon, F. Corrosion of Anodized Titanium Alloys. *Coatings* **2024**, *14*, 809. https://doi.org/10.3390/coatings14070809

Academic Editor: Maria Vittoria Diamanti

Received: 24 May 2024
Revised: 19 June 2024
Accepted: 26 June 2024
Published: 28 June 2024

1. Introduction

Midway through the 1940s, titanium alloys were created for use in aircrafts. Due to their higher density, mechanical properties, superior formability, biocompatibility, and corrosion resistance when compared to rival materials like aluminum, steel, and superalloys, two post-World War II alloys—commercially pure titanium (CPTi) and Ti-6Al-4V—remain the two most used titanium alloys in the aerospace, aeronautics, biomedical, petrochemical, chemical, and automotive industries [1–5].

The four Ti alloy types are Ti, near to, $\alpha + \beta$, and metastable, where the microstructure depends on the stabilizer (Mo, V, Cr, Ni, Fe, or Ta). Commercially pure (CP) and highly pure titanium alloys are distinguished by interstitial elements like oxygen and nitrogen, which boost titanium's mechanical resistance but reduce its ductility. Al, Zr, or Sn are added to some alloys as stabilizers for cryogenic or high-temperature applications. Near alloys have a 2% stabilizer if combined with $\alpha + \beta$ alloys' thermal solid resistance, high mechanical resistance, and other qualities. More recently, Si (0.1%–0.5%) is added to enhance their high-temperature capabilities [6–8]. $\alpha + \beta$ alloys can feature more than one stabilizer phase, such as interstitial, and can have up to 6% of these phases. Ti-6Al-4V is the most widely used Ti alloy worldwide, accounting for over 50% of production [8]. Ti alloys can have a martensitic microstructure and a high percentage of stabilizers. The microstructure may, therefore, be more complicated [8,9].

Titanium and its alloys have properties against corrosion superior to other metals because titanium generates an oxide layer of natural TiO_2. However, the environment where the alloys work can provoke a corrosion process by a break in the passive layer because it does not develop in a uniform way (especially when the alloy has different phases), generating a break and regeneration of the passive layer, but making them susceptible to corrosion attacks [10–16]. Some authors have related the chemical composition of alloys with the properties of the passive layer; adding elements such as Mn, Va, and/or Al reduces the protective properties of the oxide layer. On the other hand, elements such as Pa, Ru, Mo, and/or Zr increase the protective properties [16–20]. It is important to mention that the Ti alloy microstructure plays an important role in forming the oxide layer.

In the presence of HCl and H_2SO_4, the titanium oxide layer can be dissolved, activating the degradation of the surface and making the alloy susceptible to corrosion attacks in exposed areas. Also, titanium alloys are susceptible to Cl^- ion attacks on coated and uncoated surfaces [21,22]. Titanium has been considered a metal that does not have corrosion problems. However, it is susceptible to different corrosion attacks. This review presents a bibliography of the corrosion properties of titanium and titanium anodizing in different environments and the factors that provoke the corrosion.

2. Titanium Classification

The titanium classification is based on the crystallographic structure of alloys. This is due to the allotropic properties of titanium, with a crystalline structure, hexagonal close-packed (HCP) when it is at least than 882 °C (α phase). Ti over 882 °C presents a body-centered cubic structure (BCC) known as the β phase. However, in a pure state, maintaining the β phase is difficult, and the titanium trend returns to the α phase. To keep the β phase at low temperature, it is necessary to add different elements (β stabilizers), and the percentage of β stabilizer determines the type of Ti alloy. Different authors have classified α, near to α, α + β, β metastable, and β stable titanium [23]. Figure 1 shows the diagram of titanium and its alloys.

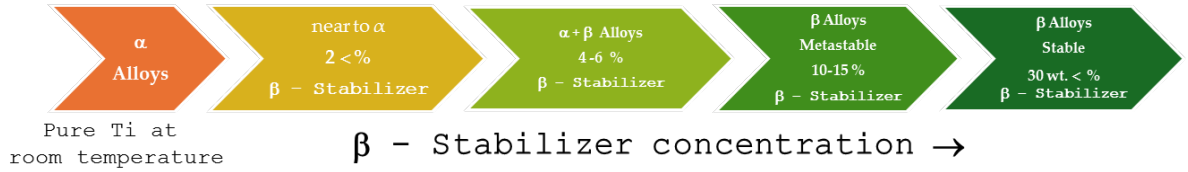

Figure 1. Diagram of titanium and its alloys.

Figure 2 shows how the different elements and β stabilizers can change the behavior of phase diagrams because some βs are isomorphous (V, Mo, Nb, Ta, and Re), and Cr, Fe, Ni, Mn, Ni, Co, Si, Fe, and Cu are eutectoids, changing the microstructure of the alloy [24–26]. The α stabilizers increase the temperature and stability of the alloy so that the alloys will not present with important changes to their microstructure. On the other hand, the β stabilizer decrease the transformation temperature to conserve the β phase, thermically working [24,27,28].

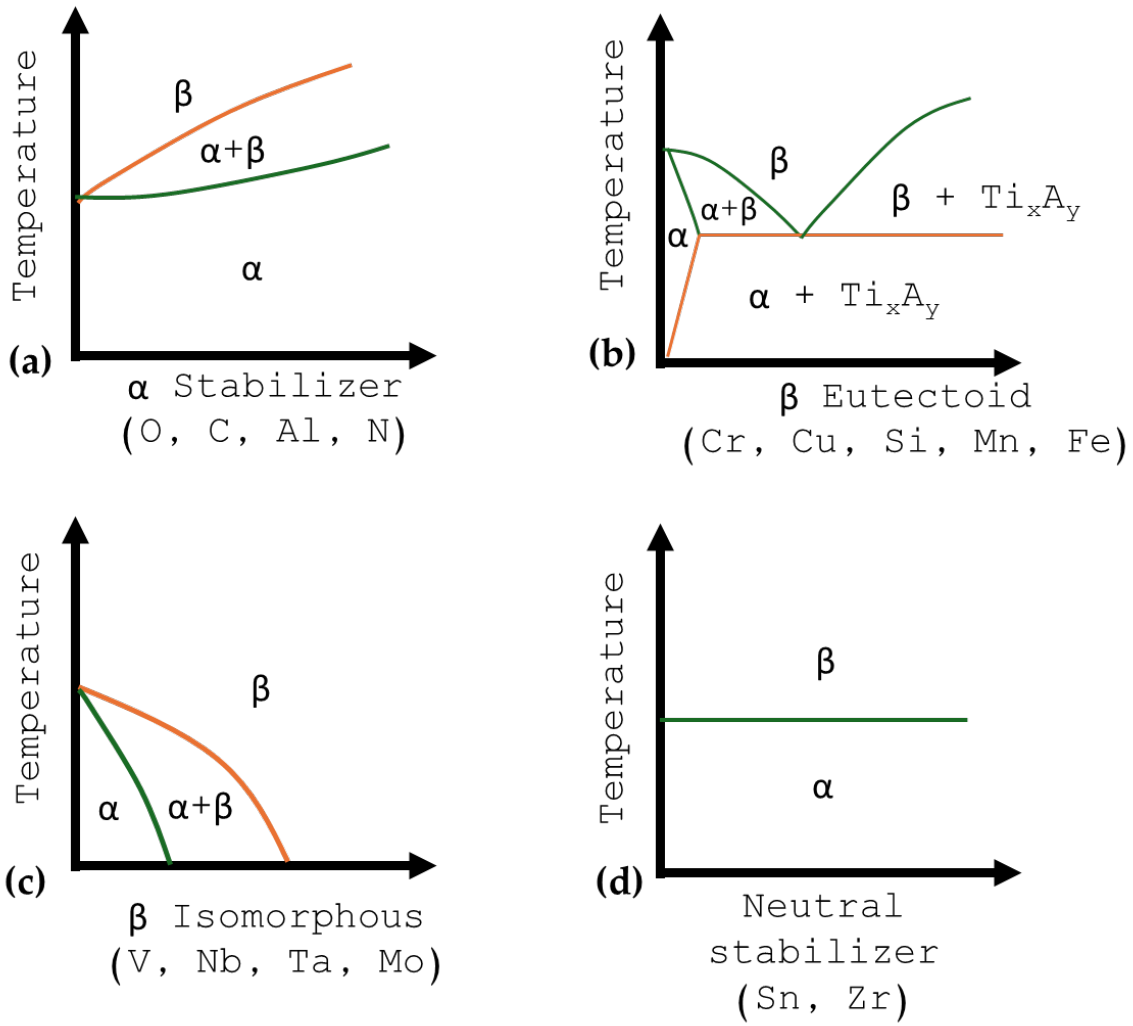

Figure 2. Phase diagrams for different elements: (**a**) α stabilizer, (**b**) β eutectoid, (**c**) β isomorphous, and (**d**) neutral stabilizer.

2.1. Titanium Alpha (α)

Usually, it is known as commercial pure (CP) and high-purity titanium. Also, α alloys can be obtained by alloying with α stabilizers such as Al or other neutral elements such as Sn and Zr (see Figure 2). CP alloys commonly present interstitial elements such as O, N, and H, and the percentage of those elements will classify the purity grade. These alloys are employed mainly in the chemical industry due to their good properties against corrosion and their ductility [24,29,30].

2.2. Titanium near to α

These alloys are employed due to their properties against high temperatures because they combine the resistance to creep in the α phase with the resistance to high stress in α + β alloys. The operation is limited to 500 to 550 °C [30–32]. The limit of the percentage of β stabilizers is 2%. The first alloy used was the Ti-8-1-1, with 8% aluminum, but the actual near to α alloys did not have 6% aluminum; this is because the alloy with 8% presented susceptibility to cracking and SCC. Some alloys have 0.1% of Si, and when employed at high temperatures use 0.5% [33,34].

2.3. Titanium α + β

These alloys have a balance between the two phases (α and β). These alloys contain one or more α stabilizers or an interstitial, and one or more β stabilizers in different percentages. α + β alloys are more susceptible to heat treatment. Usually, α + β alloys present Al between 5 and 6%, and from 4 to 6% in β stabilizers [35].

α + β alloys are the most employed in the industry. Around 70% of Ti alloys used in the world are the α + β alloys. The operating temperature of the alloys is between 350 and 450 °C [36].

2.4. Titanium Beta (β)

β alloys present low concentrations of α stabilizers, between 10 to 15% of β alloys. These alloys facilitate wide application with cool or different hardening methods. Also, their fatigue resistance is higher than that of the α + β alloys [8,9,33]. The alloys are employed in structural applications with high requirements due to the low elastic modulus and good resistance against corrosion [37,38].

When the β stabilizer is over 30%, the alloy is called β stable, but this type is not employed in any industry. The biomedical industry is studying the possibilities of implant applications due to biocompatibility [39–41].

3. Corrosion in Titanium

Titanium presents high resistance against corrosion due to the aggressive reaction of Ti with the O in the air or the aqueous solutions. The reaction generates a TiO_2 protective layer (it can present a crystalline structure or can be amorphous) of anatase or rutile. It is important to mention that recent research demonstrates that the alloying elements play an essential role in the protective properties of the Ti passive layer; elements such as Mn, Va, and Al decrease the efficiency of the protective layer. Meanwhile, Pa, Ru, Mo, and Zr increase the protective layer properties [42].

Authors have reported that the reduced acids (HCl and H_2SO_4) dissolve the titanium oxide layers, activating the degradation at contact with the surface and making the alloy susceptible to corrosion attacks in the uncovered zones. Also, Ti alloys presented susceptibility to pitting attacks by Cl^- ions in contact with metal and coating [43,44].

Another factor that influences Ti alloy corrosion is the variation in pH electrolytes. This can increase the corrosion rate of material due to the change in the potential corrosion (E_{corr}), which can provoke the dissolution of the oxide layer. Another important factor is the temperature, because pH and temperature determine the properties of the oxide layer, changing parameters such as porosity, adherence, and thickness, just to mention some of the most important. Also, the regeneration of the passive layer after a localized attack is influenced by pH and temperature of the electrolyte [45–48].

When the pH is localized in acid environments (down 4), the oxide layers are dissolved, converting the titanium into a susceptible and active metal (eliminating the passivity) at potentials between 0.7 and 0.3 V vs. SCE. The composite that damages the Ti is the H_2Ti; if the electrolysis process generates that composite, the corrosion kinetic will increase [48].

When Ti presents a potential equal to or higher than −0.3 V vs. SCE, the titanium will be passive, generating oxygen evolution on the surface; if the alloys are α and exposed to those potentials, breaking the passive layer is very difficult. However, if the alloy presents elements as Al, V, or Mn, a localized process will probably occur on the surface. In chloride environments, the energy necessary to begin a corrosion process is higher, so the corrosion occurs as an interstitial process, and the porosities will attack it. When the temperatures increase to 70 °C, the passive layers will be weak and more porous [42,49–51].

3.1. Corrosion Mechanisms

Also, corrosion can be classified into different types; aqueous corrosion processes will have two fundamental reactions. When the conditions are anaerobic, the water will convert into an oxidant agent, creating metal oxides, hydroxides, or hydratase oxides with gaseous hydrogen according to Equation (1) [52–54]:

$$M + n \cdot H_2O \leftrightarrow M(OH)_n + \frac{n}{2} \cdot H_2 \quad (1)$$

The aerobics reactions when oxygen is the oxidizing agent are similar to Equation (1), but in this case, the hydrogen formation did not occur, as Equation (2) shows [42,55]:

$$M + n \cdot H_2O + \frac{n}{2} \cdot O_2 \leftrightarrow M(OH)_{2n} \quad (2)$$

The autoprotolysis in the corrosion system can change pH concentration, affecting the material surface or coating. Also, both reactions can occur simultaneously; the aerobic reaction occurs in a preferent way, so the material will present a trend to passivation and higher corrosion resistance [56].

Different corrosion types can occur on Ti, which can be uniform, localized (crevice or pitting), caused by stress, fatigue, hydrogen, or tribocorrosion. Figure 3 shows the Pourbaix diagram; when Ti is not hydrated, Figure 3a, the passive zone is higher than when it is hydrated, Figure 3b. When it is hydrated, the corrosion zone increases from pH 0 to 8. In the corrosion zone, there is an unstable TiO_2 layer that can be dissolved even in acid and basic pH. Therefore, Ti is considered vulnerable to corrosion when the potential is negative and oxygen reduction occurs [57–60]. The dashed lines (orange color) in Figure 3 indicate the potential dependence of the hydrogen "a" and the oxygen "b" electrodes.

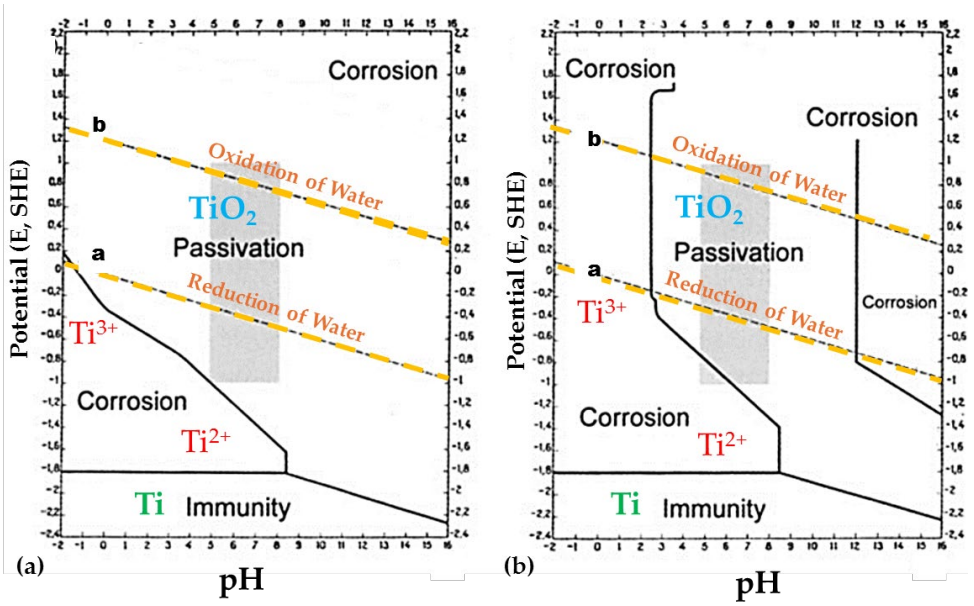

Figure 3. Pourbaix diagram of titanium in the presence of water at 25 °C: (**a**) Ti is not hydrated (**b**) Ti hydrated [58].

A uniform attack on the material surface characterizes uniform corrosion. This type of corrosion can be presented in preferential zones because some corrosion products can localize in some zones. Uniform corrosion can present on Ti when the temperature and the acid concentration increase, dissolving the oxide layer and creating a metal ion soluble as in the next equation [57,61].

$$Ti \rightarrow Ti^{3+} + 3e^- \quad (3)$$

With Ti^{3+} being more unstable than Ti^{4+}, the unstable forms of Ti are II and III. The basic reaction equation of Ti corrosion is Equation (4). However, the Ti^{4+} is uncommon in aqueous solutions due to the high charge density that occurs by the deprotonation of OH- ions. From this, the stable layer of $TiO_2 \cdot nH_2O$ is generated [62,63].

$$Ti + 4H_2O \leftrightarrow Ti(OH)_4 + 2H_2 \quad (4)$$

3.2. Crevice Corrosion

The crevice corrosion is the most common in Ti alloys. Various authors consider this corrosion localized because it occurs in a zone with a metal–metal interface that avoids oxygen reduction. This is damaging because if H^+ ions are free to interact with electrons, the pH can be reduced, causing a material dissolution. Crevice corrosion is very common in union and paint zones; the principal causative of the degradation is the diffusion of Cl^- and OH^- ions because of anodic–cathodic reactions [58,64,65].

The crevice corrosion theory consists of the necessity of energy for the corrosion process. According to Fontana, the mechanism that acts can be divided into different stages. The first stage (Equations (5) and (6)) consists of anodic and cathodic reaction that occurs inside and out of the crevice, where the ions are balanced electrostatically by OH^- ions. In the second stage, the cathodic reaction consumes the crevice's oxygen. In the third stage, the diffusion process begins; in this case, Cl^- is taken as an example. The Cl^- and OH^- ions are diffused into the crevice, decreasing the system's energy and forming a metallic chloride. Equation (7) explains the metal chloride hydrolysis at low pH inside the crevice. Finally, in the fourth stage, the M^+ and Cl^- ions decrease the pH of the crevice, increasing the material dissolution by generating more metal ions [55,56].

$$M \rightarrow M^{n+} \quad (5)$$

$$O_2 + 2H_2O + 4e^- \rightarrow 4OH^- \quad (6)$$

$$MCl_n + nH_2O \rightarrow M(OH)_n + nHCl \quad (7)$$

Equation (7) describes the process of metal and chloride ions, resulting in the chloride acid and hydroxide of the metal being very aggressive on the surface [62]. This type of corrosion limits the application of titanium in all industries due to the complex process. Betts and Boulton [66] resume the crevice corrosion reaction according to the media that occurs in Table 1.

Table 1. Reactions according to the crevice corrosion in different media [66].

Media	Reaction
Acid (oxygen reduction)	$O_2 + 4H^+ + 4e^- \rightarrow 2H_2O$
Neutral/alkaline (oxygen reduction)	$O_2 + 2H_2O + 4e^- \rightarrow 4OH^-$
Chloride reduction (acid)	$Cl_2 + 2e^- \rightarrow 2Cl^-$
Hypochlorite reduction (near to neutral)	$HClO + H^+ + 2e^- \rightarrow 2H_2O + Cl^-$
Hypochlorite reduction (alkaline)	$Cl^- + H_2O + 2e^- \rightarrow 2OH^- + Cl^-$
Sulfur reduction	$S + 2H^+ + 4e^- \rightarrow H_2S$
Thiosulfate reduction	$S_2O_3^{2-} + 6H^+ + 4e^- \rightarrow 2S + 3H_2O$
Hydrogen evolution (discharge)	$2H^+ + 2e^- \rightarrow H_2$
Hydrogen evolution (neutral/alkaline)	$2H_2O + 2e^- \rightarrow H_2 + 2OH^-$

Figure 4 shows the scheme of crevices' corrosion. The barrier can be painted, another metal (noble), or anodized. It is very important to mention that the mechanism inside the crevice is very similar to the pitting mechanism, with the difference that in the pitting corrosion, it is not probable that an oxygen reduction changes the pH of the solution [67].

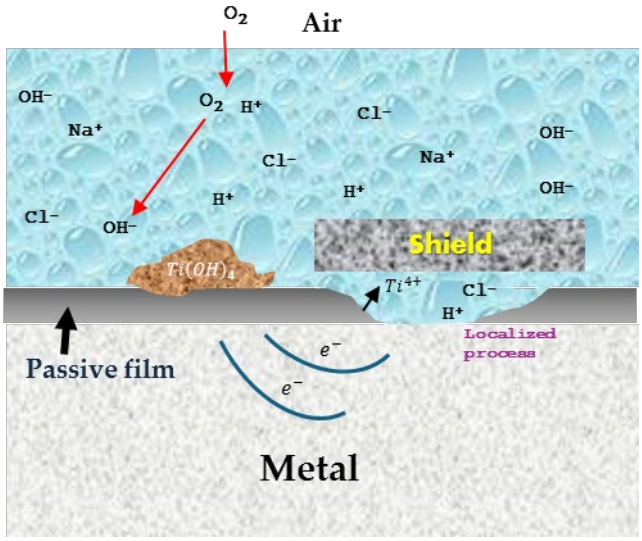

Figure 4. Scheme of crevices' corrosion.

3.3. Pitting Corrosion

Pitting corrosion occurs in passive metal due to an aggressive attack on anions. The halides are the principal causative of pitting corrosion on the oxide layer, provoking material dissolution in the zone of localized attack. The Cl^- ion is the principal pitting generator in a marine environment, but it is not exclusive to the marine environment, highway (deicing salt), food, and chemical industry. There are four pitting stages: The first is the passive layer breaking, followed by pitting nucleation, growth and repassivation. The corrosion mechanism will depend on material and environmental conditions [68].

The passive layer-breaking mechanism and the crevice corrosion are similar processes. Figure 5 shows the division of the pitting process caused by Cl^- and SO_4^- to NaCl and H_2SO_4. The scheme suggests the passive layer will break, exposing a metal zone to ions. Finally, in the adsorption phase, ions are adsorptive in the metal–oxide layer interface, accelerating the metal's and passive layer's dissolution [69–74].

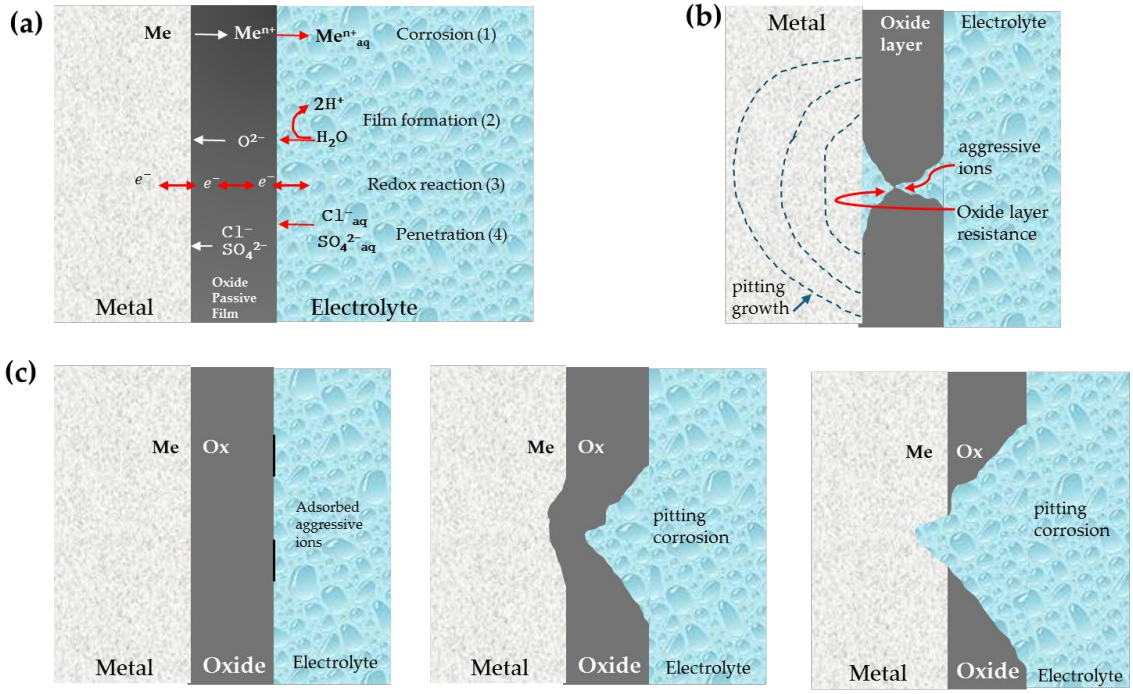

Figure 5. Pitting formation process: (**a**) electrochemical nucleation, (**b**) oxide layer breaking, and (**c**) ions adsorption mechanism [74].

Macdonald et al. [75–77] developed a repassivation and passive layer-breaking model due to the oxide layer vacancies. They assumed that the cations go from the oxide–electrolyte interface to that of the metal–oxide, generating a mass transfer process. The Cl^- can affect the vacancy diffusion process [78].

4. Coatings

Different coatings can be applied to increase the titanium corrosion resistance. Techniques such as thermal oxidation, sol–gel, sputtering, electrodeposition, passivation, and anodizing have been used to generate a resistance oxide layer [79–81]. The problem with the passivation process is the coating's low thickness, generating an oxide layer with heterogeneities; a heterogeneous layer is susceptible to localized attacks. The oxide film accomplished by the sol–gel technique is rich in Ti-OH and it has a thickness lower than 10 μm [82,83]. Plasma electrolytic oxidation (PEO) is another method that can be very effective, but the requirement of special equipment and the difficulty of processing big pieces increase the manufacturing cost. An excellent option to generate oxide layers is anodization. This process can generate a more uniform coating than that obtained by passivation. Moreover, anodization reduces the cost of finished products compared to PEO because it can be applied to big pieces [44,83–87]. The anodization technique is a fast and low-cost technique that allows for a more effortless and uniform growth of the passive layer, giving good control of its thickness, composition, and morphology [88–94].

4.1. Anodizing

The anodizing process is an electrochemical treatment to improve the artificial growth of the oxide layer in the metal surface, creating a micrometric oxide layer. This oxide layer is formed on metals when the current and/or potential are optimized. In Ti alloys, the anodizing can be in Ti^{4+} or Ti^{3+}, the last one being the most stable in solid dissolution with O^{2-} or OH^- anions, forming in the oxide–solution interface with H^+ evolution from H_2O [95,96].

To propitiate the ion migration through the oxide layer, a large electrical field must be applied, allowing for the oxide layer to grow. The high electric field can be provoked by the potential decrease caused by the metal oxide properties in the metal–oxide–electrolyte interface. The metal ions can sometimes be expulsed to the electrolyte as a dissolution [96–98].

Besides the oxide generated by the reaction, other secondary reactions can occur related to the alloy's chemical composition or the electrolyte; the reaction will have a significant impact on the anodizing efficiency. The alloys can present a deposition of dissolved alloying elements, creating secondary oxides [99–105].

The factors influencing the anodizing process are the potential applied, pH, current, electrolyte concentration, and temperature. To obtain a more defined structure, all the factors must be controlled, or at least one of them must be. The temperature controls the diffusion rate, and the porosity of the system and the pH control the pore size. Another variable is the time, this determines the type of layer that is generated: a unique barrier, porous, or with a nanotube array [104–106].

In fact, the electric field's intensity depends on electrolyte properties; a high electric field generates more and bigger breakdowns of the oxide layer, generating anodizing with bigger porosity diameters [107]. If the porous or nanotube diameters need to be small, it is necessary to employ organic electrolytes. Neutral and viscous electrolytes allow for the generation of large tubes [107,108]. Also, the electrolyte concentration affects the diameter of porosities and the porous structure [107,109].

It is important to mention that electrolyte concentration plays a fundamental role in the anodization; authors reported that Ti anodized in H_2SO_4 presented greater oxide layer growth at 0.5 M than at 2 M [110,111].

Barrier-type anodization forms quickly after exposition or with neutral pH. When neutral pH is employed to achieve anodization, it is more difficult to establish the potential and current because of the low ion transference in the system. The application for those electrolytes is low, and the oxide layer generated is very thin, with nanometric values. It occurs due to the low ion transfer [94,103].

On the other hand, when the oxide layer begins to be dissolved in the electrolyte, it generates a porous layer. The surface finish depends on the industry in which it will be applied. Aeronautical and aerospace industries require a porous layer. The pores or tubes will present an ordered array if the anodizing time is high. Usually, the barrier layer is situated on the base of the pores [105,112].

The barrier layer is first formed, and the pore's nucleation begins after that stage. The layer thickness will be proportional to the voltage applied or the ion transference. An ion's continuous flow stimulates the growth of the porosities, but it does not mean constant growth. The oxide layer stops growth gradually as it increases, and this is due to dielectric constant increases. Figure 6 shows the four stages of oxide growth: the (a) station shows the barrier layer created at the beginning, (b) is the porosity generation, (c) is the ordering of porosity to finish in, and (d) is a structured nanotubular array [112–114].

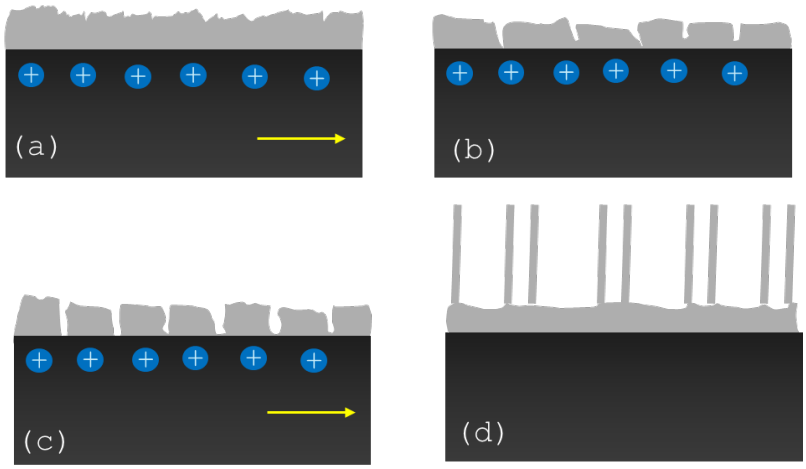

Figure 6. The 4 stages of oxide growth: (**a**) station shows the barrier layer created at beginning, (**b**) is the porosity generation, (**c**) is the ordering of porosity to finish in, and (**d**) is the structured nanotubular array.

The classic anodizing process included alkaline cleaning, activation in acid, and the anodization of the electrolyte. According to various authors, acid cleaning should be performed on HF and HNO_3 to remove TiO_2 generated naturally, as well as surface impurities such as Fe and other particles. However, standards exist that establish how to perform the anodizing, such as aeronautical standards (SAE) that suggest only an alcohol cleaning [115,116].

Kumar [117] mentioned that the H_2SO_4 electrolyte produces a stable and homogenous layer.

Authors [118,119] reported that nanotubes were formatted after 6 h at 4.5–6 pH, but other authors concluded that nanotubes could not be formed at pH greater than 6. In another study, at pH values 8–9, forming long nanotubes is more efficient than in an acid solution. Sreekantan et al. [119] support the Feng results and conclude that nanotubes can be generated at neutral pH. In that research, they found that the nanotube formation rate can be controlled by pH. Also, the crystallographic structure can be controlled by an annealing treatment. However, two types of oxides can be present (anatase and rutile).

Regardless, if the cleaning is performed with an acid or alcohol, the titanium will be the anode, and platinum the cathode. To monitor the potential, some authors have added the Ag/AgCl reference electrode [115,120]. Figure 7 shows the anodize mechanism with the respective chemical reactions and the diffusion process. The oxide layer is more resistive than the electrolyte and titanium, so the applied voltage will decrease due to the oxide [120,121].

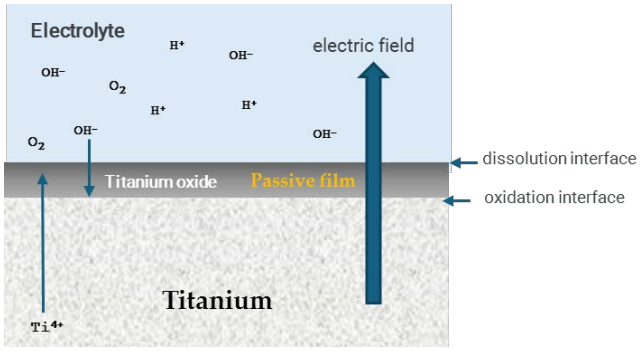

Figure 7. Anodization mechanism with the respective chemical reactions and the diffusion process.

Equations (8) and (9) describe the process that occurs in all the interfaces:

$$Ti \leftrightarrow Ti^{4+} + 4e^{-} \quad (8)$$

$$Ti^{4+} + 2H_2O \leftrightarrow TiO_2 + 4H^{+} \quad (9)$$

Various authors conclude that when two-phase Ti alloys are anodized, the oxide formation is different based on the alloy element of each phase. The α phase presents a more porous structure. Meanwhile, the β phase does not present that behavior [115,120].

The current decrease is related to the delay between the potential applied and the protective barrier under the pore. Some authors reported that an oxide with varying morphology is created when the potential decreases, generating fine pores. In contrast, a new layer is created when the potential and current increase. The anodizing efficiency increases with the potential to generate a double porous layer with a barrier layer [122,123].

Diverse authors recommend using AC to realize the anodizing. However, other authors reported that the AC anodizing in H_2SO_4 as an electrolyte generated a heterogeneous surface with sulfur deposits on low-quality porosities. Also, the AC generates a hydrogen evolution, interrupting the passive layer growth [102,124].

The current density employed directly affects pore size because of a high current increase in the electrical field. Therefore, it is normal to find different porosities when the current is changed. It is important to consider that when the current is increased, the break of the first oxide layer is more aggressive, and the formation of porosities is faster [125–127].

During anodization, it is important to consider the mass transference process and a heat transfer. Anodizing generates heat based on Joule's heating law, which explains that heat is generated due to the ionic transference in the resistive oxide layer. The temperature directly affects the oxide layer morphology; high electrolyte temperature increases porosity diameters near the oxide–electrolyte interface. This effect is caused by the high aggressiveness of electrolytes at high temperatures, accelerating the dissolution of oxide. The oxide layer thickness decreases when the metal–oxide interface is closed. The pore diameter is proportional to the voltage applied to the barrier zone [116,128].

Different authors reported that at temperatures over 40 °C, the anodizing presented an irregular surface; however, it is mechanically functional [129]. The porosity formation increases with an increase in anodizing temperatures. This is related to the viscosity of electrolytes; if the viscosity is low, the etching is faster due to faster ions' mobility. At high

viscosity, the ion transference is lower; so, at low temperatures, the pores are more irregular [130–133].

The time affects the oxide layer formation. If the anodizing time is short, pore or tube formation is impossible. To form nanotubes, it is necessary to employ at least 15 min. Porosities can be generated for 5 min (this factor will depend on electrolyte and pH). If the structure desired is porous, is necessary to anodize for a long time (more than 20 min) and use electrolytes with non-neutral pH. However, if the pH is neutral, the anodizing time will be longer (more than 1 h). The porosity will depend on the industry in which the anodizing will be applied [134,135].

4.2. Corrosion in Anodizing Titanium

The corrosion resistance that presents different titanium alloys directly depends on the alloy's chemical composition [51]. Authors such as Palka et al. [136] mentioned that material porosity influences titanium's mechanical and chemical behavior and alloys, making the material more susceptible to localized corrosion and a repassivation process [137]. For this reason, small pores propitiate the oxygen reactions, being very important to the development of TiO_2. With all the interconnected porosities, the electrolyte flow generates an easier oxygen diffusion.

The effect of the oxide layer generated can be related to the E_{corr} values. Authors such as Dabrowki et al. [138] related the increase in porosity with the passive layer, indicating that materials with less porosity presented less corrosion resistance than porous materials, increasing the E_{corr} values [139]. For this reason, and sustaining that mentioned previously, the surface finish has important relevance to the generation of the oxide layer; if surface is porous, the oxide layer generated will present better properties against corrosion than in the surface without. Some authors also related the last SiC sandpaper used to finish the material [140–143].

Although the porous metal generates a good oxide layer, is important to consider the porosity of the oxide layer, which is related to the electrolyte anodizing employed or the pH. Different processes have been reported regarding the formation of the porous layer. Ti anodized presented a cathodic–anodic behavior at CPP, it occurs when the electrolyte concentration changed due to a pH variation and an oxygen reduction. When it occurs, the protective layer is reduced by an OH^- attack; it is most common in heterogenous surface (different porosity diameters) or passivation zones [144–149].

When anodizing media is an acid such as H_3PO_4, the oxide layer is bigger and more porous. Some authors mentioned a better performance of H_3PO_4 over H_2SO_4, which is a most common anodizing electrolyte. The Ti anodized on H_3PO_4 trends to present a diffusion process due to the low ionic resistance [150–156].

Authors such as Martinez et al. [157] related the E_{corr} increase with a passive layer that does not help against corrosion. Further, an increase in passivation current density with chlorine and oxygen evolution occurs on the surface, making Ti alloys anodized and susceptible to corrosion.

When Cl^- attacks the anodized surface, the absorption will depend on the surface charge. If the surface is positively charged, the Cl^- attack will be easier when E_{corr} presents positive values. The Cl^- attacks as an interstitial element, so the anodized porosity is important. The Cl^- induces localized attacks by oxychloride accumulates in the metal–layer interface, breaking the passive layer and generating pitting corrosion [158–161].

However, alloying elements are vital because elements such as Mo, Zr, and Nb are reported to inhibit Cl^- (absorption), protecting the anodizing of Cl^- (attacks).

When evaluated with different electrochemical techniques, Ti alloys anodized with the presence of Mo presented better properties against corrosion. They commonly present with double-layer behavior.

Sadek et al. [162,163] mentioned that the formation of Ti $(OH)_x$ O_y is normal due to the oxidation process limitation by an increase in the oxide layer. The porosities propitiate the generation of the hydroxide and generate a posterior diffusion [164–166]. Nyquist's

diagrams show that hydroxide and secondary oxide generation generate a capacitive response [167].

Karambakhsh et al. [168] mentioned that the anodizing in H_2SO_4 decreased the corrosion rate due to a more stable anodic film. Also, the higher anodizing potential was associated with higher corrosion rates due to a porosity increase.

However, other authors have mentioned that an increase in anodizing voltage increases the film thickness, porosity, and crystallinity, and that anodized samples present with a reduced corrosion rate compared to non-anodized samples. However, the potential increases the porosity of titanium, and at high potentials (over 80 V), the corrosion rate will be higher at 10 V because of the anodized porosity [169,170].

The anodizing process can increase the oxide thickness to develop corrosion resistance and in turn release ions; the effect on the anodizing samples is an increase in corrosion resistance, independently of the anodizing electrolyte [171,172].

Prando et al. [173] related the potential with corrosion rate when the titanium was treated at potentials lower than 40 V, presenting better performance against corrosion. They attributed that behavior to forming one amorphous compact oxide layer, reducing the system's porosity. This information suggests that a compact oxide layer is better than a porous oxide layer against corrosion behavior.

Anodized titanium is susceptible to pitting by salt anions; the principals' anions are F^-, Cl^-, Br^-, and I^-, because it provokes a local breakdown of the protective film and initiates the pitting process [174–177]. Fluoride ions are the most aggressive halides. They form TiF_4. As Nakagawa et al. [178] researched the electrolyte pH, they indicated that samples presented passive, non-passive, and active attacks when exposed to halide solution, indicating that all the samples were susceptible to pitting attacks.

Other authors consider the Br^- ion as the most aggressive, generating localized corrosion in a range of 2.5 to 3 V vs. SCE; at 1.2 V, the redox of Br begins, and the dissolution-pitting begins [179]. The aggressive halides are Cl^-, I^-, Br^-, and F^-, with F being the most aggressive electrolyte. Also, Prando et al. [180] concluded that fluorides dissolve titanium oxide generated by anodization in H_2SO_4. Also, as chlorides do not generate localized corrosion as fluorides, the corrosion rate increases with chloride concentration because it causes the oxide layer dissolution.

Authors document that localized and uniform corrosion can occur on material surfaces. The electrochemical reaction of uniform corrosion implies that the whole area is generally slow. For localized corrosion, it occurs in preferent zones [51]. For that reason, is important to develop a uniform anodizing; if the anodizing is not completely uniform, corrosion processes can occur in specific areas (difference of porosity and morphology). Different researchers have shown that anodized morphology is very important. Anodizing in acid media presented a more uniform anodized surface than in alkaline media. The anodizing on NaOH and KOH at 1 M showed susceptibility to localized corrosion due to a non-heterogenous surface. This behavior was present in Ti-6Al-4V and Ti Beta-C. When the same alloys were anodized in H_2SO_4, they presented a homogenous surface and a trend to uniform corrosion. Additionally, other electrolytes such as alkaline media can be considered as substitutes of acid electrolytes, but it is important to mention that the anodization efficiency will not be the same.

The chemical composition of alloys plays an essential role in Ti anodization. Alloys with $\alpha + \beta$ phases commonly present more difficulty in generating a uniform oxide layer. If the β alloying element is V, it generates an unstable oxide layer. However, if the β stabilizer element is Mo or Cr, the anodic layer created in the β phase will be a more stable oxide layer. This behavior is presented in anodized Ti-6Al-4V, which can present a heterogeneous surface more susceptible to pitting than a Ti-6Al-2Sn-4Zr-2Mo alloy. The last alloy has Mo and Zr, so the anodized layer created is very stable, and anodizing is not susceptible to localized corrosion. Also, α alloys generate uniform anodized surfaces, although the corrosion rate is higher than that of alloys with Mo, Zr, or Cr elements [181–186].

The corrosion mechanism will be very different for each anodizing treatment. Figure 8 shows the different equivalent circuits obtained by ECS in different studies. The mechanism goes from a double-layer process to a Warburg diffusion process, and when anodization presents great diversity in porosities, it is normal use a three-CPE system. When the CPE α value is lower, as in Figure 8b,d, it indicates an irregular anodizing surface, with differences in porosities; on the other hand, values near to 1 indicate a homogenous surface, Figure 8a,c. The susceptibility to pitting attacks is due to hydroxide formation in the anodization, as the hydroxide layer is porous, provoking a diffusion process [90,187–194]. When the oxide layer is a small barrier (thin oxide layer), it will present the behavior shown in Figure 8a,b; the difference is the surface homogeneity. When the surface is homogeneous, the Nyquist diagram obtained will be as in Figure 8a. If the anodization presents a heterogeneous surface, the behavior is as shown in Figure 8b. On the other hand, when a double-layer system is presented, if the anodized porosity is homogenous, the α value will be near 1. The behavior presented will be similar to that in Figure 8c. In contrast, when the porosity is non-homogenous, the behavior will be similar to that in Figure 8d and the α values will be between 0.6 and 0.7.

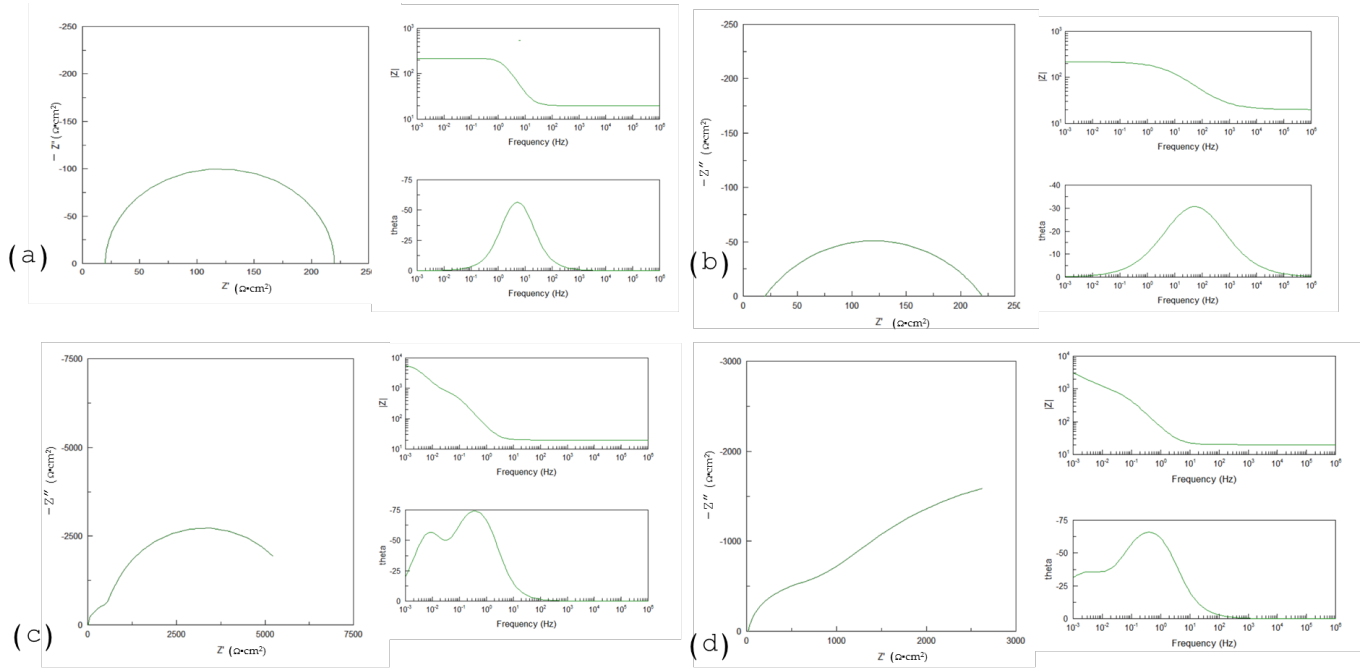

Figure 8. EIS results for (**a**) homogenous anodized surface, (**b**) heterogeneous anodized surface, (**c**) homogenous double-layer system, (**d**) second layer non-homogenous surface.

Another behavior observed in anodized Ti is shown in Figure 9a, where the equivalent circuit is similar to that in Figure 10d. That behavior is presented when the porosities have two different morphologies before arriving at a compact layer. The diffusion process is shown on Figure 9b, when the phase angle finishes on 45°, and it is related with a diffusion process. The equivalent circuit is shown in Figure 10c.

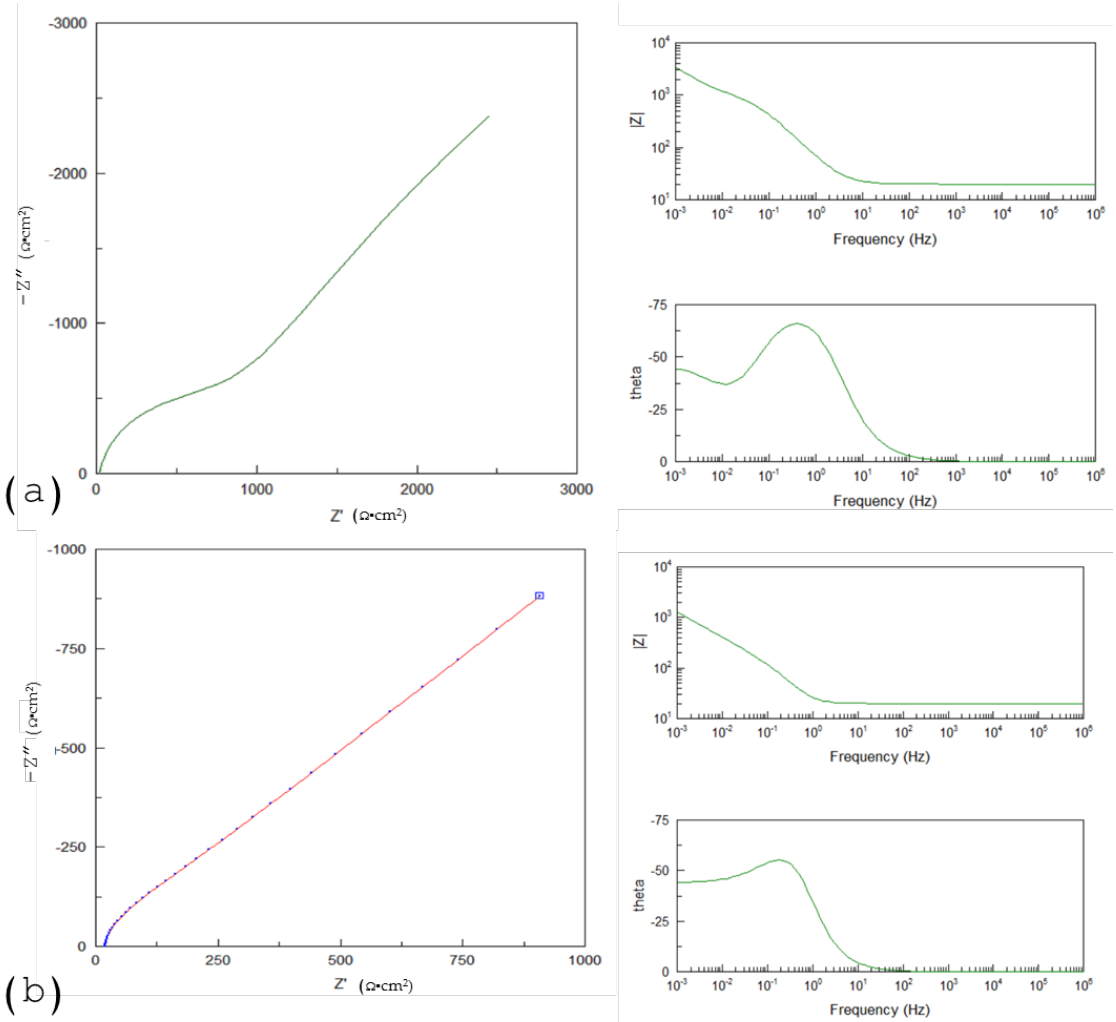

Figure 9. (**a**) Three-CPE system; (**b**) diffusion process.

Also, different authors have investigated the use of non-aggressive anodizing electrolytes such as glycerol–water; however, is necessary to add NH_4F in low percentages to facilitate the mobility of ions. Authors have reported good adherence of the oxide layer to Ti-10Mo-8Nb (β alloy) and the generation of different oxide layers such as TiO_2, MoO_2, and Nb_2O_5 [195,196]

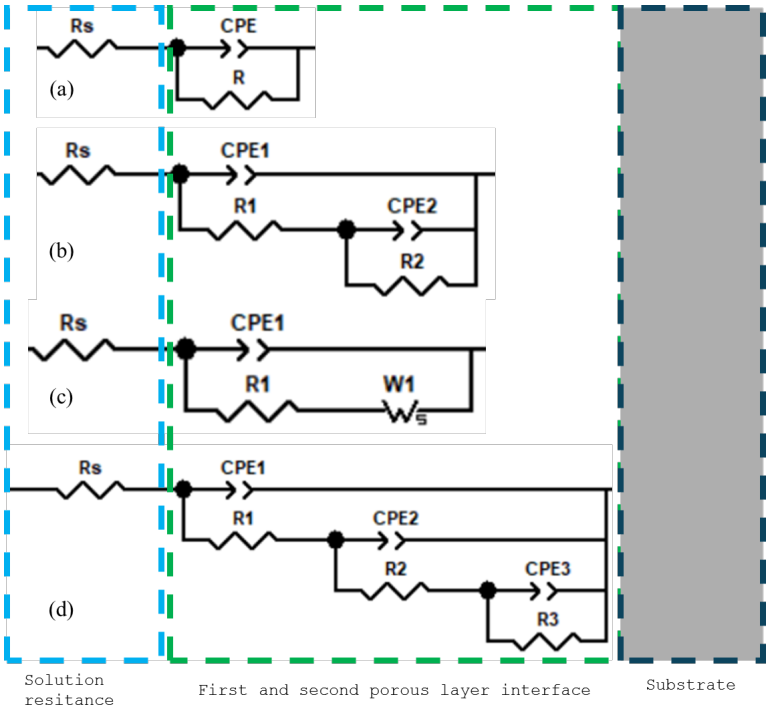

Figure 10. Equivalent circuits presented in anodized Ti samples: (**a**) a CPE system, (**b**) Two CPEs system, (**c**) a CPE system and Warburg (diffusion process); (**d**) Three CPEs system.

5. Future Directions for Anodized Titanium

Choi and Jeong [197] experimented with the generation of TiO_2 with NH4F and ethylene glycol. They found that anodizing with the highest roughness presented hydrophilicity, indicating that porosity plays an important role in electrolyte absorption [198,199]. Using glycol and relating the material surface with hydrophobics is important to future study on anodization. Choi and Jeong [196] variated the porosity with the anodizing time from 10 to 60 min each 10 min; after that, a treatment on 1H, 1H, 2H, and 2H-Perfluorooctyltrichlorosilane was realized and the transition from hydrophobic to superhydrophobic was achieved. Also, they related the corrosion resistance with the most hydrophobic sample (at 60 min).

Other researchers focus on a two-step anodizing (TSA) process, consisting of anodized Ti alloys, removing the anodization by ultrasonic cleaning and realizing the anodization again. Authors found that single-step anodization (traditional) presented more heterogeneous porosities. Two-step anodization presented less porosity, and the structure was more homogenous; this is because the gases were dissolved and prevented pore generation [200–205]. When EIS characterized TSA, it presented better resistance against corrosion with higher impedance values and a double-layer system. The TSA reduced the penetration of Cl^- ions, that is, some of the most dangerous ions for Ti alloys and anodized samples.

One of the most important uses of the anodization process for titanium is when it is applied on titanium intended for orthopedic use. The increasing use of β alloys as Ti-Ta alloys for biomedical applications indicates that it is important to conduct research on anodized samples. Different authors included this conclusion that agrees with our opinion, more for the elements with biocompatibility such as Zr, Ta, Mo, or Nb. Also, different authors report that the oxide layer generated with those elements is more stable than with V or Fe, which are β stabilizers but not biocompatible [140–143]. Using anodizing paint provides a faster and more economical option than other coating processes. With the perfect electrolyte election and determination of a good potential or current density, anodization presents a several applications for the aeronautical, aerospace, chemical, and biomedical industries.

However, it is important to mention that the anodizing surface finish will depend on the application, and we cannot say that a non-porous layer is better for anodization due to some industries such as aeronautical needing a porous surface to apply primer to the surface; however, if the anodizing is the final surface, is important to consider a non-porous surface.

6. Conclusions

This review aims to analyze an anodized layer's corrosion resistance on titanium and its alloys, with different parameters. The main conclusions are summarized as follows:

- The research results indicate that in an anodizing process, the chemical composition of the alloy is one of the first variables to be considered. The chemical composition can determine the phases of the alloy and the type of coating that will form.
    - Anodization shows better behavior against corrosion when it is carried out in acidic electrolytes. Alkaline media tend to generate a heterogeneous surface, while acidic media generate a uniform surface.
    - The biomedical industry tends to develop anodization in neutral media because a compact layer with nanometric porosities is required. One of the most used electrolytes is ethylene glycol and some anodizing salts.
    - Temperature influences anodization rates, porosity diameters, and anodization hardness. At high temperatures, it helps increase anodization rates; however, the anodization will present high porosity.
- Recent research showed that two-step anodization (TSA) performs better in developing a homogenous anodized layer than conventional anodizing. Also, the TSA presented high resistance to Cl^- ion penetration.
- To generate a thin and compact oxide layer by anodization, it is necessary to apply a voltage between 10 and 50 V. Any voltage over that range will generate porosities on the anodized surface. This anodization voltage is used for biomedical Ti alloys.
- Titanium alloys and their anodized variants will present corrosion susceptibility when exposed to solution with halides. In the environment, Cl generates a corrosion process in Ti alloys and its anodized variants.
- Elements such as V generate an oxide layer susceptible to corrosion attacks; however, elements as Zr, Mo, Nb, and Cr help to generate a more stable oxide layer that avoids the corrosion process.

Author Contributions: Conceptualization, J.M.J.-M. and F.A.-C. methodology, D.N.-M., F.E.-L., M.G.C.-R., C.T.M.-R., and M.L.-B.; data curation, M.A.B.-Z., G.S.-H., D.N.-M., C.T.M.-R., and M.L.-B.; formal analysis, F.A.-C., M.A.B.-Z., J.M.J.-M., G.S.-H., and C.G.-T.; validation, J.M.J.-M., C.G.-T., and F.A.-C.; writing—original draft preparation, J.M.J.-M., C.G.-T., and F.A.-C.; writing—review and editing, J.M.J.-M. and F.A.-C. All authors have read and agreed to the published version of the manuscript.

Funding: This research was funded by the Universidad Autónoma de Nuevo León (UANL).

Institutional Review Board Statement: Not applicable.

Informed Consent Statement: Not applicable.

Data Availability Statement: Not applicable.

Acknowledgments: The authors acknowledge the Academic Body UANL—CA-316 "Deterioration and integrity of composite materials".

Conflicts of Interest: The authors declare no conflicts of interest.

References

1. Sam Froes, F.H.; Qian, M.; Niinomi, M. An Introduction to Titanium in Consumer Applications. In *Titanium for Consumer Applications*; Elsevier: Amsterdam, The Netherlands, 2019; pp. 1–12. https://doi.org/10.1016/B978-0-12-815820-3.00001-0.
2. Sha, W.; Malinov, S. *Titanium Alloys: Modelling of Microstructure, Properties and Applications*; Elsevier Ltd.: Amsterdam, The Netherlands, 2009; ISBN 9781845693756.
3. Gialanella, S.; Malandruccolo, A. Aerospace Alloys. In *Topics in Mining, Metallurgy and Materials Engineering*; Springer International Publishing: Cham, Switzerland, 2020; ISBN 9783030244392.
4. Mouritz, A.P. *Introduction to Aerospace Materials*; Elsevier Inc.: Amsterdam, The Netherlands, 2012; ISBN 9781855739468.
5. Peñarrieta-Juanito, G.; Sordi, M.B.; Henriques, B.; Dotto, M.E.R.; Teughels, W.; Silva, F.S.; Magini, R.S.; Souza, J.C.M. *Titanium and Titanium Alloys*, 1st ed.; Leyens, C., Peters, M., Eds.; Wiley: Hoboken, NJ, USA, 2003.
6. Jáquez-Muñoz, J.M.; Gaona-Tiburcio, C.; Cabral-Miramontes, J.; Nieves-Mendoza, D.; Maldonado-Bandala, E.; Olguín-Coca, J.; López-Léon, L.D.; De Los Rios, J.P.F.; Almeraya-Calderón, F. Electrochemical Noise Analysis of the Corrosion of Titanium Alloys in NaCl and H_2SO_4 Solutions. *Metals* **2021**, *11*, 105. https://doi.org/10.3390/MET11010105.
7. Chien, C.S.; Hung, Y.C.; Hong, T.F.; Wu, C.C.; Kuo, T.Y.; Lee, T.M.; Liao, T.Y.; Lin, H.C.; Chuang, C.H. Preparation and Characterization of Porous Bioceramic Layers on Pure Titanium Surfaces Obtained by Micro-Arc Oxidation Process. *Appl. Phys. A Mater. Sci. Process.* **2017**, *123*, 204. https://doi.org/10.1007/s00339-017-0765-0.
8. Yang, X.; Liu, C.R. Machining Titanium and Its Alloys. *Mach. Sci. Technol.* **1999**, *3*, 107–139. https://doi.org/10.1080/10940349908945686.
9. Semiatin, S.L.; Seetharaman, V.; Weiss, I. The Thermomechanical Processing of Alpha/Beta Titanium Alloys; *Miner. Met. Mater. Soc.* **1997**, *49*, 33–39.
10. Contu, F.; Elsener, B.; Böhni, H. A Study of the Potentials Achieved during Mechanical Abrasion and the Repassivation Rate of Titanium and Ti_6Al_4V in Inorganic Buffer Solutions and Bovine Serum. *Electrochim. Acta* **2004**, *50*, 33–41. https://doi.org/10.1016/J.ELECTACTA.2004.07.024.
11. Peñarrieta-Juanito, G.; Sordi, M.B.; Henriques, B.; Dotto, M.E.R.; Teughels, W.; Silva, F.S.; Magini, R.S.; Souza, J.C.M. Surface Damage of Dental Implant Systems and Ions Release after Exposure to Fluoride and Hydrogen Peroxide. *J. Periodontal Res.* **2019**, *54*, 46–52. https://doi.org/10.1111/JRE.12603.
12. Sharma, A.; Oh, M.C.; Kim, J.T.; Srivastava, A.K.; Ahn, B. Investigation of Electrochemical Corrosion Behavior of Additive Manufactured Ti–6Al–4V Alloy for Medical Implants in Different Electrolytes. *J. Alloys Compd.* **2020**, *830*, 154620. https://doi.org/10.1016/J.JALLCOM.2020.154620.
13. Cordeiro, J.M.; Barão, V.A.R. Is There Scientific Evidence Favoring the Substitution of Commercially Pure Titanium with Titanium Alloys for the Manufacture of Dental Implants? *Mater. Sci. Eng. C* **2017**, *71*, 1201–1215. https://doi.org/10.1016/J.MSEC.2016.10.025.
14. Mehkri, S.; Abishek, N.R.; Sumanth, K.S.; Rekha, N. Study of the Tribocorrosion Occurring at the Implant and Implant Alloy Interface: Dental Implant Materials. *Mater. Today Proc.* **2021**, *44*, 157–165. https://doi.org/10.1016/J.MATPR.2020.08.550.
15. Apaza-Bedoya, K.; Tarce, M.; Benfatti, C.A.M.; Henriques, B.; Mathew, M.T.; Teughels, W.; Souza, J.C.M. Synergistic Interactions between Corrosion and Wear at Titanium-Based Dental Implant Connections: A Scoping Review. *J. Periodontal Res.* **2017**, *52*, 946–954. https://doi.org/10.1111/JRE.12469.
16. Dini, C.; Costa, R.C.; Sukotjo, C.; Takoudis, C.G.; Mathew, M.T.; Barão, V.A.R. Progression of Bio-Tribocorrosion in Implant Dentistry. *Front. Mech. Eng.* **2020**, *6*, 497882. https://doi.org/10.3389/FMECH.2020.00001/BIBTEX.
17. Diercks, D.R.; Loomis, B.A. Alloying and Impurity Effects in Vanadium-Base Alloys. *J. Nucl. Mater.* **1986**, *141–143*, 1117–1124. https://doi.org/10.1016/0022-3115(86)90152-2.
18. Meng, Y.; Cui, J.; Zhao, Z.; Zuo, Y. Effect of Vanadium on the Microstructures and Mechanical Properties of an Al–Mg–Si–Cu–Cr–Ti Alloy of 6XXX Series. *J. Alloys Compd.* **2013**, *573*, 102–111. https://doi.org/10.1016/J.JALLCOM.2013.03.239.
19. Shen, J.; Nagasaka, T.; Tokitani, M.; Muroga, T.; Kasada, R.; Sakurai, S. Effects of Titanium Concentration on Microstructure and Mechanical Properties of High-Purity Vanadium Alloys. *Mater. Des.* **2022**, *224*, 111390. https://doi.org/10.1016/J.MATDES.2022.111390.
20. Najafi, H.; Rassizadehghani, J. Effects of Vanadium and Titanium on Mechanical Properties of Low Carbon as Cast Microalloyed Steels. *Int. J. Cast. Met. Res.* **2006**, *19*, 323–329. https://doi.org/10.1179/136404606X163505.
21. Vaughan, J.; Alfantazi, A. Corrosion of Titanium and Its Alloys in Sulfuric Acid in the Presence of Chlorides. *J. Electrochem. Soc.* **2006**, *153*, B6. https://doi.org/10.1149/1.2126580/XML.
22. Vasilescu, C.; Drob, S.I.; Osiceanu, P.; Calderon-Moreno, J.M.; Drob, P.; Vasilescu, E. Characterisation of Passive Film and Corrosion Behaviour of a New Ti-Ta-Zr Alloy in Artificial Oral Media: In Time Influence of pH and Fluoride Ion Content. *Mater. Corros.* **2015**, *66*, 971–981. https://doi.org/10.1002/MACO.201408025.
23. Pushp, P.; Dasharath, S.M.; Arati, C. Classification and Applications of Titanium and Its Alloys. *Mater. Today Proc.* **2022**, *54*, 537–542. https://doi.org/10.1016/J.MATPR.2022.01.008.
24. Yadav, P.; Saxena, K.K. Effect of Heat-Treatment on Microstructure and Mechanical Properties of Ti Alloys: An Overview. *Mater. Today Proc.* **2020**, *26*, 2546–2557. https://doi.org/10.1016/J.MATPR.2020.02.541.
25. Tendero Lozano, I. *Desarrollo de Aleaciones de Titanio-Manganeso Pulvimetalúrgicas Para Aplicaciones Biomédicas*; Universitat Politècnica de València: Valencia, Spain, 2018.

26. Veiga, C.; Davim, J.P.; Loureiro, A.J.R. Loureiro Properties and Applications of Titanium Alloys: A Brief Review. *Rev. Adv. Mater. Sci.* **2012**, *32*, 133–148.
27. Lütjering, G.; Williams, J.C. *Titanium*; Engineering Materials, Processes; Springer: Berlin/Heidelberg, Germany, 2007; ISBN 978-3-540-71397-5.
28. Abe, J.O.; Popoola, A.P.I.; Popoola, O.M. Influence of Varied Process Parameters on the Microstructure, Densification and Microhardness of Spark Plasma Sintered Ti-6Al-4V/h-BN Binary Composite. *IOP Conf. Ser. Mater. Sci. Eng.* **2019**, *689*, 012005. https://doi.org/10.1088/1757-899X/689/1/012005.
29. Ahmed, Y.M.; Salleh, K.; Sahari, M.; Ishak, M.; Khidhir, B.A. Titanium and Its Alloy. *Int. J. Sci. Res.* **2014**, *3*, 1351–1361.
30. Donachie, M.J. *Titanium—A Technical Guide*; ASM International: Detroit, MI, USA, 2000; Volume 55, ISBN 978-0-87170-686-7.
31. Kuphasuk, C.; Oshida, Y.; Andres, C.J.; Hovijitra, S.T.; Barco, M.T.; Brown, D.T. Electrochemical Corrosion of Titanium and Titanium-Based Alloys. *J. Prosthet. Dent.* **2001**, *85*, 195–202.
32. Pathania, A.; Kumar, S.A.; Nagesha, B.K.; Barad, S.; Suresh, T.N. Reclamation of Titanium Alloy Based Aerospace Parts Using Laser Based Metal Deposition Methodology. *Mater. Today Proc.* **2021**, *45*, 4886–4892. https://doi.org/10.1016/J.MATPR.2021.01.354.
33. Peel, C.J.; Gregson, P.J. Design Requirements for Aerospace Structural Materials. In *High Performance Materials in Aerospace*; Springer: Dordrecht, The Netherlands, 1995; pp. 1–48. https://doi.org/10.1007/978-94-011-0685-6_1.
34. Barrington, N.; Black, M. Aerospace Materials and Manufacturing Processes at the Millennium. In *Aerospace Materials*; CRC Press: Boca Raton, FL, USA, 2020; Volume 1, pp. 15–26. https://doi.org/10.1201/9781420034721-3/AEROSPACE-MATERIALS-MANUFACTURING-PROCESSES-MILLENNIUM-BRIAN-CANTOR-ASSENDER-GRANT.
35. Dutta Majumdar, J.; Manna, I. Laser Surface Engineering of Titanium and Its Alloys for Improved Wear, Corrosion and High-Temperature Oxidation Resistance. In *Laser Surface Engineering: Processes and Applications*; Woodhead Publishing: Sawston, UK, 2015; pp. 483–521, ISBN 9781782420798.
36. Banerjee, D.; Williams, J.C. Perspectives on Titanium Science and Technology. *Acta Mater.* **2013**, *61*, 844–879. https://doi.org/10.1016/j.actamat.2012.10.043.
37. Sankaran, K.K.; Mishra, R.S. *Metallurgy and Design of Alloys with Hierarchical Microstructures*; Elsevier Inc.: Amsterdam, The Netherlands, 2017; ISBN 9780128120255.
38. Bermingham, M.J.; StJohn, D.H.; Krynen, J.; Tedman-Jones, S.; Dargusch, M.S. Promoting the Columnar to Equiaxed Transition and Grain Refinement of Titanium Alloys during Additive Manufacturing. *Acta Mater.* **2019**, *168*, 261–274. https://doi.org/10.1016/J.ACTAMAT.2019.02.020.
39. Kolli, R.P.; Devaraj, A. A Review of Metastable Beta Titanium Alloys. *Metals* **2018**, *8*, 506. https://doi.org/10.3390/MET8070506.
40. Bambach, M.D.; Seifert, D.; Sizova, I. Intensive Forming of Grade 5 Titanium Bars with Increased Performance for Aerospace Applications. *Procedia Manuf.* **2020**, *47*, 288–294.
41. Bermingham, M.J.; Kent, D.; Pace, B.; Cairney, J.M.; Dargusch, M.S. High Strength Heat-Treatable β-Titanium Alloy for Additive Manufacturing. *Mater. Sci. Eng. A* **2020**, *791*, 139646. https://doi.org/10.1016/J.MSEA.2020.139646.
42. Bodunrin, M.O.; Chown, L.H.; Van Der Merwe, J.W.; Alaneme, K.K.; Oganbule, C.; Klenam, D.E.P.; Mphasha, N.P. Corrosion Behavior of Titanium Alloys in Acidic and Saline Media: Role of Alloy Design, Passivation Integrity, and Electrolyte Modification. *Corros. Rev.* **2020**, *38*, 25–47. https://doi.org/10.1515/CORRREV-2019-0029/ASSET/GRAPHIC/J_CORRREV-2019-0029_CV_007.JPG.
43. Jáquez-Muñoz, J.M.; Gaona-Tiburcio, C.; Méndez-Ramírez, C.T.; Baltazar-Zamora, M.Á.; Estupinán-López, F.; Bautista-Margulis, R.G.; Cuevas-Rodríguez, J.; Flores-De los Rios, J.P.; Almeraya-Calderón, F. Corrosion of Titanium Alloys Anodized Using Electrochemical Techniques. Metals **2023**, 13, 476. https://doi.org/10.3390/met13030476.
44. Vasilescu, C.; Drob, S.I.; Neacsu, E.I.; Mirza Rosca, J.C. Surface Analysis and Corrosion Resistance of a New Titanium Base Alloy in Simulated Body Fluids. *Corros. Sci.* **2012**, *65*, 431–440. https://doi.org/10.1016/J.CORSCI.2012.08.042.
45. Castany, P.; Gordin, D.M.; Drob, S.I.; Vasilescu, C.; Mitran, V.; Cimpean, A.; Gloriant, T. Deformation Mechanisms and Biocompatibility of the Superelastic Ti–23Nb–0.7Ta–2Zr–0.5N Alloy. *Shape Mem. Superelasticity* **2016**, *2*, 18–28. https://doi.org/10.1007/S40830-016-0057-0/FIGURES/7.
46. Vasilescu, C.; Drob, S.I.; Osiceanu, P.; Moreno, J.M.C.; Prodana, M.; Ionita, D.; Demetrescu, I.; Marcu, M.; Popovici, I.A.; Vasilescu, E. Microstructure, Surface Characterization, and Electrochemical Behavior of New Ti-Zr-Ta-Ag Alloy in Simulated Human Electrolyte. *Metall. Mater. Trans. A Phys. Metall. Mater. Sci.* **2017**, *48*, 513–523. https://doi.org/10.1007/S11661-016-3774-2/TABLES/5.
47. Coakley, J.; Vorontsov, V.A.; Littrell, K.C.; Heenan, R.K.; Ohnuma, M.; Jones, N.G.; Dye, D. Nanoprecipitation in a Beta-Titanium Alloy. *J. Alloys Compd.* **2015**, *623*, 146–156. https://doi.org/10.1016/J.JALLCOM.2014.10.038.
48. Wandelt, K. *Encyclopedia of Interfacial Chemistry*; Elsevier: Amsterdam, The Netherlands, 2018.
49. Brandoli, B.; de Geus, A.R.; Souza, J.R.; Spadon, G.; Soares, A.; Rodrigues, J.F.; Komorowski, J.; Matwin, S. Aircraft Fuselage Corrosion Detection Using Artificial Intelligence. *Sensors* **2021**, *21*, 4026. https://doi.org/10.3390/S21124026.
50. Coakley, J.; Isheim, D.; Radecka, A.; Dye, D.; Stone, H.J.; Seidman, D.N. Microstructural Evolution in a Superelastic Metastable Beta-Ti Alloy. *Scr. Mater.* **2017**, *128*, 87–90. https://doi.org/10.1016/J.SCRIPTAMAT.2016.09.035.
51. Bocchetta, P.; Chen, L.Y.; Tardelli, J.D.C.; Dos Reis, A.C.; Almeraya-Calderón, F.; Leo, P. Passive Layers and Corrosion Resistance of Biomedical Ti-6Al-4V and β-Ti Alloys. *Coatings* **2021**, *11*, 487. https://doi.org/10.3390/COATINGS11050487.
52. Schweitzer, P.E. *Paint and Coatings*; CRC Press: Boca Raton, FL, USA, 2005; Volume 35.

53. Schweitzer, P.E.P.A. *Corrosion Engineering Handbook—3 Volume Set*; CRC Press: Boca Raton, FL, USA, 2018; ISBN 9780429188084.
54. Revie, R.W.; Uhlig, H.H. *Corrosion and Corrosion Control: An Introduction to Corrosion Science and Engineering*, 4th ed.; John Wiley and Sons: Hoboken, NJ, USA, 2008; ISBN 9780471732792.
55. Hebert, K.; Alkire, R. Dissolved Metal Species Mechanism for Initiation of Crevice Corrosion of Aluminum: II. *Math. Model. J. Electrochem. Soc.* **1983**, *130*, 1007–1014. https://doi.org/10.1149/1.2119875/XML.
56. Rashidi, N.; Alavi-Soltani, S.R.; Asmatulu, R. *Crevice Corrosion Theory, Mechanisms and Prevention Methods*; Wichita State University. Graduate School: Wichita, KS, USA, 2007.
57. Alves, A.C.; Wenger, F.; Ponthiaux, P.; Celis, J.P.; Pinto, A.M.; Rocha, L.A.; Fernandes, J.C.S. Corrosion Mechanisms in Titanium Oxide-Based Films Produced by Anodic Treatment. *Electrochim. Acta* **2017**, *234*, 16–27. https://doi.org/10.1016/J.ELECTACTA.2017.03.011.
58. Rodrigues, D.C.; Valderrama, P.; Wilson, T.G.; Palmer, K.; Thomas, A.; Sridhar, S.; Adapalli, A.; Burbano, M.; Wadhwani, C. Titanium Corrosion Mechanisms in the Oral Environment: A Retrieval Study. *Materials* **2013**, *6*, 5258–5274. https://doi.org/10.3390/ma6115258.
59. Zieliński, A.; Sobieszczyk, S. Corrosion of Titanium Biomaterials, Mechanisms, Effects and Modelisation. *Corros. Rev.* **2008**, *26*, 1–22. https://doi.org/10.1515/CORRREV.2008.1/MACHINEREADABLECITATION/RIS.
60. Pourbaix, M.; Burbank, J. Atlas D-Equilibres Electrochimiques. *J. Electrochem. Soc.* **1964**, *111*, 14C. https://doi.org/10.1149/1.2426051.
61. Demo, J.; Friedersdorf, F. Aircraft Corrosion Monitoring and Data Visualization Techniques for Condition Based Maintenance. In Proceedings of the 2015 IEEE Aerospace Conference, Big Sky, MT, USA, 8 June 2015. https://doi.org/10.1109/AERO.2015.7119048.
62. Schenk, R. *The Corrosion Properties of Titanium and Titanium Alloys*; Springer: Berlin/Heidelberg, Germany, 2001; pp. 145–170.
63. Rodrigues, D.C.; Urban, R.M.; Jacobs, J.J.; Gilbert, J.L. In Vivo Severe Corrosion and Hydrogen Embrittlement of Retrieved Modular Body Titanium Alloy Hip-Implants. *J. Biomed. Mater. Res. B Appl. Biomater.* **2009**, *88*, 206–219. https://doi.org/10.1002/JBM.B.31171.
64. Laurindo, C.A.H.; Torres, R.D.; Mali, S.A.; Gilbert, J.L.; Soares, P. Incorporation of Ca and P on Anodized Titanium Surface: Effect of High Current Density. *Mater. Sci. Eng. C* **2014**, *37*, 223–231. https://doi.org/10.1016/J.MSEC.2014.01.006.
65. Chaturvedi, T.P. An Overview of the Corrosion Aspect of Dental Implants (Titanium and Its Alloys). *Indian J. Dent. Res.* **2009**, *20*, 91–98. https://doi.org/10.4103/0970-9290.49068.
66. Betts, A.J.; Boulton, L.H. Crevice Corrosion: Review of Mechanisms, Modelling, and Mitigation. *Br. Corros. J.* **1993**, *28*, 279–295. https://doi.org/10.1179/000705993799156299.
67. Makhlouf, A.S.H.; Botello, M.A. Failure of the Metallic Structures Due to Microbiologically Induced Corrosion and the Techniques for Protection. In *Handbook of Materials Failure Analysis*; Butterworth-Heinemann: Oxford, UK, 2018; pp. 1–18. https://doi.org/10.1016/B978-0-08-101928-3.00001-X.
68. Strehblow, H.H.; Marcus, P. Mechanisms of Pitting Corrosion. In *Corrosion Mechanisms in Theory and Practice*, 3th ed.; CRC Press: Boca Raton, FL, USA, 2011; pp. 349–394, ISBN 9781420094633.
69. Sato, N.; Kudo, K.; Noda, T. The Anodic Oxide Film on Iron in Neutral Solution. *Electrochim. Acta* **1971**, *16*, 1909–1921. https://doi.org/10.1016/0013-4686(71)85146-0.
70. Sato, N. A Theory for Breakdown of Anodic Oxide Films on Metals. *Electrochim. Acta* **1971**, *16*, 1683–1692. https://doi.org/10.1016/0013-4686(71)85079-X.
71. Galvele, J.R. 1-Pitting Corrosion. *Treatise Mater. Sci. Technol.* **1983**, *23*, 1–57.
72. Soltis, J. Passivity Breakdown, Pit Initiation and Propagation of Pits in Metallic Materials—Review. *Corros. Sci.* **2015**, *90*, 5–22. https://doi.org/10.1016/J.CORSCI.2014.10.006.
73. Frankel, G.S. Pitting Corrosion of Metals: A Review of the Critical Factors. *J. Electrochem. Soc.* **1998**, *145*, 2186–2198. https://doi.org/10.1149/1.1838615/XML.
74. Isaacs, H.S. The Localized Breakdown and Repair of Passive Surfaces during Pitting. *Corros. Sci.* **1989**, *29*, 313–323. https://doi.org/10.1016/0010-938X(89)90038-3.
75. Chao, C.Y.; Lin, L.F.; Macdonald, D.D. A Point Defect Model for Anodic Passive Films: III. Impedance Response. *J. Electrochem. Soc.* **1982**, *129*, 1874–1879. https://doi.org/10.1149/1.2124318/XML.
76. Macdonald, D.D. The Point Defect Model for the Passive State. *J. Electrochem. Soc.* **1992**, *139*, 3434–3449. https://doi.org/10.1149/1.2069096/XML.
77. Macdonald, D.D. Review of Mechanistic Analysis by Electrochemical Impedance Spectroscopy. *Electrochim. Acta* **1990**, *35*, 1509–1525. https://doi.org/10.1016/0013-4686(90)80005-9.
78. Engelhardt, G.R.; Macdonald, D.D. Monte-Carlo Simulation of Pitting Corrosion with a Deterministic Model for Repassivation. *J. Electrochem. Soc.* **2020**, *167*, 013540. https://doi.org/10.1149/1945-7111/AB67A0.
79. Alam, M.J.; Cameron, D.C. Preparation and Characterization of TiO_2 Thin Films by Sol-Gel Method. *J. Sol.-Gel. Sci. Technol.* **2002**, *25*, 137–145. https://doi.org/10.1023/A:1019912312654.
80. Diamanti, M.V.; Codeluppi, S.; Cordioli, A.; Pedeferri, M.P. Effect of Thermal Oxidation on Titanium Oxides' Characteristics. *J. Exp. Nanosci.* **2009**, *4*, 365–372. https://doi.org/10.1080/17458080902769937.
81. Löbl, P.; Huppertz, M.; Mergel, D. Nucleation and Growth in TiO_2 Films Prepared by Sputtering and Evaporation. *Thin Solid. Film.* **1994**, *251*, 72–79. https://doi.org/10.1016/0040-6090(94)90843-5.

82. Dziewoński, P.M.; Grzeszczuk, M. Deposition of Thin TiO_2 Layers on Platinum by Means of Cyclic Voltammetry of Selected Complex Ti(IV) Media Leading to Anatase. *Electrochim. Acta* **2009**, *54*, 4045–4055. https://doi.org/10.1016/j.electacta.2009.02.036.
83. Ma, K.; Zhang, R.; Sun, J.; Liu, C. Oxidation Mechanism of Biomedical Titanium Alloy Surface and Experiment. *Int. J. Corros.* **2020**, *2020*, 1678615. https://doi.org/10.1155/2020/1678615.
84. Benea, L.; Celis, J.P. Reactivity of Porous Titanium Oxide Film and Chitosan Layer Electrochemically Formed on Ti-6Al-4V Alloy in Biological Solution. *Surf. Coat. Technol.* **2018**, *354*, 145–152. https://doi.org/10.1016/J.SURFCOAT.2018.09.015.
85. Li, Q.; Zhang, Y.; Cheng, Y.; Zuo, X.; Wang, Y.; Yuan, X.; Huang, H. Effect of Temperature on the Corrosion Behavior and Corrosion Resistance of Copper–Aluminum Laminated Composite Plate. *Materials* **2022**, *15*, 1621. https://doi.org/10.3390/MA15041621.
86. Blasco-Tamarit, E.; Igual-Muñoz, A.; Antón, J.G.; García-García, D.M. Galvanic Corrosion of Titanium Coupled to Welded Titanium in LiBr Solutions at Different Temperatures. *Corros. Sci.* **2009**, *51*, 1095–1102. https://doi.org/10.1016/J.CORSCI.2009.02.023.
87. Takemoto, S.; Hattori, M.; Yoshinari, M.; Kawada, E.; Oda, Y. Corrosion Behavior and Surface Characterization of Titanium in Solution Containing Fluoride and Albumin. *Biomaterials* **2005**, *26*, 829–837. https://doi.org/10.1016/J.BIOMATERIALS.2004.03.025.
88. Almeraya-Calderon, F.; Villegas-Tovar, M.; Maldonado-Bandala, E.; Lara-Banda, M.; Baltazar-Zamora, M.A.; Santiago-Hurtado, G.; Nieves-Mendoza, D.; Lopez-Leon, L.D.; Jaquez-Muñoz, J.M.; Estupiñán-López, F.; et al. Use of Electrochemical Noise for the Study of Corrosion by Passivated CUSTOM 450 and AM 350 Stainless Steels. *Metals* **2024**, 14, 341. https://doi.org/10.3390/met14030341.
89. Michalska-Domańska, M.; Łazińska, M.; Łukasiewicz, J.; Mol, J.M.C.; Durejko, T. Self-Organized Anodic Oxides on Titanium Alloys Prepared from Glycol- and Glycerol-Based Electrolytes. *Materials* **2020**, *13*, 4743. https://doi.org/10.3390/MA13214743.
90. Guo, T.; Ivanovski, S.; Gulati, K. Fresh or Aged: Short Time Anodization of Titanium to Understand the Influence of Electrolyte Aging on Titania Nanopores. *J. Mater. Sci. Technol.* **2022**, *119*, 245–256. https://doi.org/10.1016/J.JMST.2021.11.050.
91. Gulati, K.; Aw, M.S.; Findlay, D.; Losic, D. Local Drug Delivery to the Bone by Drug-Releasing Implants: Perspectives of Nano-Engineered Titania Nanotube Arrays. *Ther. Deliv.* **2012**, *3*, 857–873. https://doi.org/10.4155/TDE.12.66.
92. Luz, A.R.; Santos, L.S.; Lepienski, C.M.; Kuroda, P.B.; Kuromoto, N.K. Characterization of the Morphology, Structure and Wettability of Phase Dependent Lamellar and Nanotube Oxides on Anodized Ti-10Nb Alloy. *Appl. Surf. Sci.* **2018**, *448*, 30–40. https://doi.org/10.1016/J.APSUSC.2018.04.079.
93. Dikici, T.; Erol, M.; Toparli, M.; Celik, E. Characterization and Photocatalytic Properties of Nanoporous Titanium Dioxide Layer Fabricated on Pure Titanium Substrates by the Anodic Oxidation Process. *Ceram. Int.* **2014**, *40*, 1587–1591. https://doi.org/10.1016/J.CERAMINT.2013.07.046.
94. Montoya-Rangel, M; Garza-Montes-de-Oca, N; Gaona-Tiburcio, C; Almeraya-Calderón,F. Corrosion mechanism of advanced high strength dual-phase steels by electrochemical noise analysis in chloride solutions, *Mater. Today Commun*., Volume 35, 2023,105663, https://doi.org/10.1016/j.mtcomm.2023.105663
95. Thompson, G.E. Porous Anodic Alumina: Fabrication, Characterization and Applications. *Thin Solid Film.* **1997**, *297*, 192–201. https://doi.org/10.1016/S0040-6090(96)09440-0.
96. Xu, Y.; Thompson, G.E.; Wood, G.C.; Bethune, B. Anion Incorporation and Migration during Barrier Film Formation on Aluminium. *Corros. Sci.* **1987**, *27*, 83–102. https://doi.org/10.1016/0010-938X(87)90121-1.
97. Saenz de Miera, M.; Curioni, M.; Skeldon, P.; Thompson, G.E. The Behaviour of Second Phase Particles during Anodizing of Aluminium Alloys. *Corros. Sci.* **2010**, *52*, 2489–2497. https://doi.org/10.1016/J.CORSCI.2010.03.029.
98. Saenz de Miera, M.; Curioni, M.; Skeldon, P.; Thompson, G.E. Modelling the Anodizing Behaviour of Aluminium Alloys in Sulphuric Acid through Alloy Analogues. *Corros. Sci.* **2008**, *50*, 3410–3415. https://doi.org/10.1016/J.CORSCI.2008.09.019.
99. Martínez-Viademonte, M.P.; Abrahami, S.T.; Hack, T.; Burchardt, M.; Terryn, H. A Review on Anodizing of Aerospace Aluminum Alloys for Corrosion Protection. *Coatings* **2020**, *10*, 1106. https://doi.org/10.3390/COATINGS10111106.
100. Mazzarolo, A.; Curioni, M.; Vicenzo, A.; Skeldon, P.; Thompson, G.E. Anodic Growth of Titanium Oxide: Electrochemical Behaviour and Morphological Evolution. *Electrochim. Acta* **2012**, *75*, 288–295. https://doi.org/10.1016/J.ELECTACTA.2012.04.114.
101. Torrescano-Alvarez, J.M.; Curioni, M.; Skeldon, P. Effects of Oxygen Evolution on the Voltage and Film Morphology during Galvanostatic Anodizing of AA 2024-T3 Aluminium Alloy in Sulphuric Acid at −2 and 24 °C. *Electrochim. Acta* **2018**, *275*, 172–181. https://doi.org/10.1016/J.ELECTACTA.2018.03.121.
102. Ono, S.; Ichinose, H.; Kawaguchi, T.; Masuko, N. The Observation of Anodic Oxide Films on Aluminum by High Resolution Electron Microscopy. *Corros. Sci.* **1990**, *31*, 249–254. https://doi.org/10.1016/0010-938X(90)90115-L.
103. Palibroda, E.; Marginean, P. Considerations on the Adsorbed Water Concentration of Sulfuric Porous Aluminium Oxide. *Thin Solid Film.* **1994**, *240*, 73–75. https://doi.org/10.1016/0040-6090(94)90697-1.
104. Voon, C.H.; Derman, M.N.; Hashim, U.; Ahmad, K.R.; Foo, K.L. Effect of Temperature of Oxalic Acid on the Fabrication of Porous Anodic Alumina from Al-Mn Alloys. *J. Nanomater.* **2013**, *2013*, 167047. https://doi.org/10.1155/2013/167047.
105. Lee, W.; Park, S.J. Porous Anodic Aluminum Oxide: Anodization and Templated Synthesis of Functional Nanostructures. *Chem. Rev.* **2014**, *114*, 7487–7556. https://doi.org/10.1021/CR500002Z/ASSET/IMAGES/CR500002Z.SOCIAL.JPEG_V03.
106. Cao, S.; Zhou, X.; Lim, C.V.S.; Boyer, R.R.; Williams, J.C.; Wu, X. A Strong and Ductile Ti-3Al-8V-6Cr-4Mo-4Zr (Beta-C) Alloy Achieved by Introducing Trace Carbon Addition and Cold Work. *Scr. Mater.* **2020**, *178*, 124–128. https://doi.org/10.1016/J.SCRIPTAMAT.2019.11.021.

107. Taveira, L.V.; Macák, J.M.; Tsuchiya, H.; Dick, L.F.P.; Schmuki, P. Initiation and Growth of Self-Organized TiO_2 Nanotubes Anodically Formed in NH4F/ (NH4) 2SO4 Electrolytes. *J. Electrochem. Soc.* **2005**, *152*, B405. https://doi.org/10.1149/1.2008980.
108. Tsuchiya, H.; Macak, J.M.; Taveira, L.; Balaur, E.; Ghicov, A.; Sirotna, K.; Schmuki, P. Self-Organized TiO_2 Nanotubes Prepared in Ammonium Fluoride Containing Acetic Acid Electrolytes. *Electrochem. Commun.* **2005**, *7*, 576–580. https://doi.org/10.1016/J.ELECOM.2005.04.008.
109. Tsuchiya, H.; Kurokawa, T.; Miyabe, S.; Fujimoto, S. Fast Current-Controlled Polarization for the Analysis of Rapid Cathodic Process on Anodized Metal. *J. Electrochem. Soc.* **2019**, *166*, C3443–C3447. https://doi.org/10.1149/2.0501911JES/XML.
110. Guerra Neto, C.L.B.; Da Silva, M.A.M.; Alves, C. In Vitro Study of Cell Behaviour on Plasma Surface Modified Titanium. *Surf. Eng.* **2009**, *25*, 146–150. https://doi.org/10.1179/174329408X271561.
111. Prando, D.; Brenna, A.; Diamanti, M.V.; Beretta, S.; Bolzoni, F.; Ormellese, M.; Pedeferri, M.P. Corrosion of Titanium: Part 2: Effects of Surface Treatments. *J. Appl. Biomater. Funct. Mater.* **2018**, *16*, 3–13. https://doi.org/10.5301/JABFM.5000396/ASSET/IMAGES/LARGE/10.5301_JABFM.5000396-FIG9.JPEG.
112. Salman, S.A.; Okido, M. Anodization of Magnesium (Mg) Alloys to Improve Corrosion Resistance. *Corros. Prev. Magnes. Alloys* **2013**, 197–231. https://doi.org/10.1533/9780857098962.2.197.
113. David, T.M.; Priya, D.R.; Wilson, P.; Sagayaraj, P.; Mathews, T. A Critical Review on the Variations in Anodization Parameters toward Microstructural Formation of TiO_2 Nanotubes. *Electrochem. Sci. Adv.* **2022**, *2*, e202100083. https://doi.org/10.1002/ELSA.202100083.
114. Raj, V.; Rajaram, M.P.; Balasubramanian, G.; Vincent, S.; Kanagaraj, D. Pulse Anodizing—An Overview. *Trans. IMF* **2017**, *81*, 114–121. https://doi.org/10.1080/00202967.2003.11871515.
115. İzmir, M.; Ercan, B. Anodization of Titanium Alloys for Orthopedic Applications. *Front. Chem. Sci. Eng.* **2019**, *13*, 28–45. https://doi.org/10.1007/S11705-018-1759-Y/METRICS.
116. Aerts, T.; Jorcin, J.B.; De Graeve, I.; Terryn, H. Comparison between the Influence of Applied Electrode and Electrolyte Temperatures on Porous Anodizing of Aluminium. *Electrochim. Acta* **2010**, *55*, 3957–3965. https://doi.org/10.1016/J.ELECTACTA.2010.02.044.
117. Kumar, A. Anodization of Titanium Alloy (Grade 5) to Obtain Nanoporous Surface Using Sulfuric Acid Electrolyte. *IETE J. Res.* **2020**, *68*, 3855–3861. https://doi.org/10.1080/03772063.2020.1780958.
118. Olmo Martinez, R.D.; Munirathinam, B.; Michalska-Domańska, M. Biomedical Application of Anodic Nanomaterials. *Synth. Bionano. Mater. Biomed. Appl.* **2023**, 395–441. https://doi.org/10.1016/B978-0-323-91195-5.00022-2.
119. Sreekantan, S.; Lockman, Z.; Hazan, R.; Tasbihi, M.; Tong, L.K.; Mohamed, A.R. Influence of Electrolyte pH on TiO_2 Nanotube Formation by Ti Anodization. *J. Alloys Compd.* **2009**, *485*, 478–483. https://doi.org/10.1016/J.JALLCOM.2009.05.152.
120. Yao, C.; Webster, T.J. Anodization: A Promising Nano-Modification Technique of Titanium Implants for Orthopedic Applications. *J. Nanosci. Nanotechnol.* **2006**, *6*, 2682–2692. https://doi.org/10.1166/JNN.2006.447.
121. Minagar, S.; Wang, J.; Berndt, C.C.; Ivanova, E.P.; Wen, C. Cell Response of Anodized Nanotubes on Titanium and Titanium Alloys. *J. Biomed. Mater. Res. Part A* **2013**, *101A*, 2726–2739. https://doi.org/10.1002/jbm.a.34575.
122. Samaniego-Gámez, P.; Almeraya-Calderón, F.; Martin, U.; Ress, J.; Gaona-Tiburcio, C.; Silva-Vidaurri, L.; Cabral-Miramontes, J.; Bastidas, J.M.; Chacón-Nava, J.G.; Bastidas, D.M. Efecto del tratamiento de sellado en el comportamiento frente a corrosión de la aleación anodizada de aluminio-litio AA2099. *Rev. Met.* **2020**, *56*, e180. https://doi.org/10.3989/revmetalm.180.
123. De Graeve, I.; Terryn, H.; Thompson, G.E. AC-Anodising of Aluminium: Contribution to Electrical and Efficiency Study. *Electrochim. Acta* **2006**, *52*, 1127–1134. https://doi.org/10.1016/J.ELECTACTA.2006.07.010.
124. Chung, C.K.; Liao, M.W.; Chang, H.C.; Lee, C.T. Effects of Temperature and Voltage Mode on Nanoporous Anodic Aluminum Oxide Films by One-Step Anodization. *Thin Solid Film.* **2011**, *520*, 1554–1558. https://doi.org/10.1016/J.TSF.2011.08.053.
125. Allam, N.K.; Grimes, C.A. Effect of Cathode Material on the Morphology and Photoelectrochemical Properties of Vertically Oriented TiO_2 Nanotube Arrays. *Sol. Energy Mater. Sol. Cells* **2008**, *92*, 1468–1475. https://doi.org/10.1016/J.SOLMAT.2008.06.007.
126. Indira, K.; Ningshen, S.; Mudali, U.K.; Rajendran, N. Effect of Anodization Parameters on the Structural Morphology of Titanium in Fluoride Containing Electrolytes. *Mater. Charact.* **2012**, *71*, 58–65. https://doi.org/10.1016/J.MATCHAR.2012.06.005.
127. Tsuchiya, H.; Macak, J.M.; Ghicov, A.; Räder, A.S.; Taveira, L.; Schmuki, P. Characterization of Electronic Properties of TiO_2 Nanotube Films. *Corros. Sci.* **2007**, *49*, 203–210. https://doi.org/10.1016/J.CORSCI.2006.05.009.
128. Abd-Elnaiem, A.M.; Gaber, A. Parametric Study on the Anodization of Pure Aluminum Thin Film Used in Fabricating Nano-Pores Template. *Int. J. Electrochem. Sci.* **2013**, *8*, 9741–9751.
129. Macak, J.M.; Tsuchiya, H.; Taveira, L.; Aldabergerova, S.; Schmuki, P. Smooth Anodic TiO_2 Nanotubes. *Angew. Chem. Int. Ed.* **2005**, *44*, 7463–7465. https://doi.org/10.1002/ANIE.200502781.
130. Wang, J.; Lin, Z. Anodic Formation of Ordered TiO_2 Nanotube Arrays: Effects of Electrolyte Temperature and Anodization Potential. *J. Phys. Chem. C* **2009**, *113*, 4026–4030. https://doi.org/10.1021/JP811201X.
131. Chen, X.; Chen, J.; Lin, J. Self-Assembled TiO_2 Nanotube Arrays with U-Shaped Profile by Controlling Anodization Temperature. *J. Nanomater.* **2010**, *2010*, 753253. https://doi.org/10.1155/2010/753253.
132. Mohan, L.; Dennis, C.; Padmapriya, N.; Anandan, C.; Rajendran, N. Effect of Electrolyte Temperature and Anodization Time on Formation of TiO_2 Nanotubes for Biomedical Applications. *Mater. Today Commun.* **2020**, *23*, 101103. https://doi.org/10.1016/J.MTCOMM.2020.101103.

133. Yun, K.C.; Chen, Y.C.; Kuo, M.Y.; Wang, H.W.; Lu, Y.F.; Chung, J.C.; Liu, Y.C.; Zeng, Y.Z. Synthesis and Characterization of Highly Ordered TiO_2 Nanotube Arrays for Hydrogen Generation via Water Splitting. *Mater. Chem. Phys.* **2011**, *129*, 35–39. https://doi.org/10.1016/J.MATCHEMPHYS.2011.03.081.
134. Li, Y.; Ma, Q.; Han, J.; Ji, L.; Wang, J.; Chen, J.; Wang, Y. Controllable Preparation, Growth Mechanism and the Properties Research of TiO_2 Nanotube Arrays. *Appl. Surf. Sci.* **2014**, *297*, 103–108. https://doi.org/10.1016/J.APSUSC.2014.01.086.
135. Joo, S.; Muto, I.; Hara, N. In Situ Ellipsometric Analysis of Growth Processes of Anodic TiO_2 Nanotube Films. *J. Electrochem. Soc.* **2008**, *155*, C154. https://doi.org/10.1149/1.2837859/XML.
136. Pałka, K.; Pokrowiecki, R.; Krzywicka, M. Porous Titanium Materials and Applications. In *Titanium for Consumer Applications: Real-World Use of Titanium*; Elsevier: Amsterdam, The Netherlands, 2019; pp. 27–75, ISBN 9780128158203.
137. Eah, K.H.W.; Thampuran, R.; Teoh, S.H. The Influence of Pore Morphology on Corrosion. *Corros. Sci.* **1998**, *40*, 547–556. https://doi.org/10.1016/S0010-938X(97)00152-2.
138. Dabrowski, B.; Kaminski, J.; Swieszkowski, W.; Kurzydlowski, K.J. Porous Titanium Scaffolds for Biomedical Applications: Corrosion Resistance and Structure Investigation. *Mater. Sci. Forum* **2011**, *674*, 41–46. https://doi.org/10.4028/www.scientific.net/MSF.674.41.
139. Chen, X.; Fu, Q.; Jin, Y.; Li, M.; Yang, R.; Cui, X.; Gong, M. In Vitro Studying Corrosion Behavior of Porous Titanium Coating in Dynamic Electrolyte. *Mater. Sci. Eng. C* **2017**, *70*, 1071–1075. https://doi.org/10.1016/j.msec.2016.03.044.
140. Ye, D.; Wang, W.; Xu, Z.; Yin, C.; Zhou, H.; Li, Y. Prediction of Thermal Barrier Coatings Microstructural Features Based on Support Vector Machine Optimized by Cuckoo Search Algorithm. *Coatings* **2020**, *10*, 704. https://doi.org/10.3390/COATINGS10070704.
141. Karballaeezadeh, N.; Danial, M.S.; Moazemi, D.; Band, S.S.; Mosavi, A.; Reuter, U. Smart Structural Health Monitoring of Flexible Pavements Using Machine Learning Methods. *Coatings* **2020**, *10*, 1100. https://doi.org/10.3390/COATINGS10111100.
142. Singh, A.V.; Jahnke, T.; Wang, S.; Xiao, Y.; Alapan, Y.; Kharratian, S.; Onbasli, M.C.; Kozielski, K.; David, H.; Richter, G.; et al. Anisotropic Gold Nanostructures: Optimization via in Silico Modeling for Hyperthermia. *ACS Appl. Nano Mater.* **2018**, *1*, 6205–6216. https://doi.org/10.1021/ACSANM.8B01406/SUPPL_FILE/AN8B01406_SI_001.PDF.
143. Thampi, V.V.A.; Ramanathan, S. Corrosion Behavior of Anodized Ti-Ta Binary Surface Alloys in Various Physiological Fluids for Implant Applications. *Corros. Sci.* **2023**, *219*, 111233. https://doi.org/10.1016/J.CORSCI.2023.111233.
144. Cabral-Miramontes, J.A.; Bastidas, D.M.; Baltazar, M.A.; Zambrano-Robledo, P.; Bastidas, J.M.; Almeraya-Calderón, F.M.; Gaona-Tiburcio, C. Corrosion Behavior of Zn-TiO_2 and Zn-ZnO Electrodeposited Coatings in 3.5% NaCl Solution. *Int. J. Electrochem. Sci.* **2019**, *14*, 4226–4239. https://doi.org/10.20964/2019.05.10.
145. Jaquez-Muñoz, J.; Gaona-Tiburcio, C.; Lira-Martinez, A.; Zambrano-Robledo, P.; Maldonado-Bandala, E.; Samaniego-Gamez, O.; Nieves-Mendoza, D.; Olguin-Coca, J.; Estupiñan-Lopez, F.; Almeraya-Calderon, F. Susceptibility to Pitting Corrosion of Ti-CP2, Ti-6Al-2Sn-4Zr-2Mo, and Ti-6Al-4V Alloys for Aeronautical Applications. *Metals* **2021**, *11*, 1002. https://doi.org/10.3390/met11071002.
146. Eavers, J.A.; Durr, C.L.; Thompson, N.G. Unique Interpretations of Potentiodynamic Polarization Technique. In Proceedings of the NACE—International Corrosion Conference Series, San Diego, CA, USA, 22–27 March 1998.
147. Cabral Miramontes, J.A.; Barceinas Sánchez, J.D.O.; Almeraya Calderón, F.; Martínez Villafañe, A.; Chacón Nava, J.G. Effect of Boron Additions on Sintering and Densification of a Ferritic Stainless Steel. *J. Mater. Eng. Perform.* **2010**, *19*, 880–884.
148. Ramgopal, T.; Schmutz, P.; Frankel, G.S. Electrochemical Behavior of Thin Film Analogs of Mg(Zn, Cu, Al) [Sub 2]. *J. Electrochem. Soc.* **2001**, *148*, B348. https://doi.org/10.1149/1.1386626/XML.
149. Montoya-Rangel, M.; de Oca, N.G.M.; Gaona-Tiburcio, C.; Colás, R.; Cabral-Miramontes, J.; Nieves-Mendoza, D.; Maldonado-Bandala, E.; Chacón-Nava, J.; Almeraya-Calderón, F. Electrochemical Noise Measurements of Advanced High-Strength Steels in Different Solutions. *Metals* **2020**, *10*, 1232. https://doi.org/10.3390/MET10091232.
150. Ispas, A.; Bund, A.; Vrublevsky, I. Investigations on Current Transients in Porous Alumina Films during Re-Anodizing Using the Electrochemical Quartz Crystal Microbalance. *J. Solid State Electrochem.* **2010**, *14*, 2121–2128. https://doi.org/10.1007/S10008-010-1043-7/METRICS.
151. Huang, Y.S.; Shih, T.S.; Chou, J.H. Electrochemical Behavior of Anodized AA7075-T73 Alloys as Affected by the Matrix Structure. *Appl. Surf. Sci.* **2013**, *283*, 249–257. https://doi.org/10.1016/J.APSUSC.2013.06.094.
152. Zaraska, L.; Gawlak, K.; Gurgul, M.; Dziurka, M.; Nowak, M.; Gilek, D.; Sulka, G.D. Influence of Anodizing Conditions on Generation of Internal Cracks in Anodic Porous Tin Oxide Films Grown in NaOH Electrolyte. *Appl. Surf. Sci.* **2018**, *439*, 672–680. https://doi.org/10.1016/J.APSUSC.2017.12.188.
153. Gawalt, E.S.; Brault-Rios, K.; Dixon, M.S.; Tang, D.C.; Schwartz, J. Enhanced Bonding of Organometallics to Titanium via a Titanium(III) Phosphate Interface. *Langmuir* **2001**, *17*, 6743–6745. https://doi.org/10.1021/la010595r.
154. Khudhair, D.; Bhatti, A.; Li, Y.; Hamedani, H.A.; Garmestani, H.; Hodgson, P.; Nahavandi, S. Anodization Parameters Influencing the Morphology and Electrical Properties of TiO_2 Nanotubes for Living Cell Interfacing and Investigations. *Mater. Sci. Eng. C* **2016**, *59*, 1125–1142.
155. El-Taib Heakal, F.; Mogoda, A.S.; Mazhar, A.A.; El-Basiouny, M.S. Kinetic Studies on the Dissolution of the Anodic Oxide Film on Titanium in Phosphoric Acid Solutions. *Corros. Sci.* **1987**, *27*, 453–462. https://doi.org/10.1016/0010-938X(87)90089-8.
156. Parse, H.; Patil, I.M.; Swami, A.S.; Kakade, B.A. TiO_2-Decorated Titanium Carbide MXene Co-Doped with Nitrogen and Sulfur for Oxygen Electroreduction. *ACS Appl. Nano Mater.* **2021**, *4*, 1094–1103. https://doi.org/10.1021/ACSANM.0C02695/SUPPL_FILE/AN0C02695_SI_001.PDF.

157. Martínez-Ramos, C.; Olguin-Coca, J.; Lopez-Leon, L.D.; Gaona-Tiburcio, C.; Lara-Banda, M.; Maldonado-Bandala, E.; Castañeda-Robles, I.; Jaquez-Muñoz, J.M.; Cabral-Miramontes, J.; Nieves-Mendoza, D.; F. Almeraya-Calderón. Electrochemical Noise Analysis Using Experimental Chaos Theory, Power Spectral Density and Hilbert–Huang Transform in Anodized Aluminum Alloys in Tartaric–Phosphoric–Sulfuric Acid Solutions. Metals **2023**, 13, 1850. https://doi.org/10.3390/met13111850.
158. Legat, A.; Doleček, V. Corrosion Monitoring System Based on Measurement and Analysis of Electrochemical Noise. *Corrosion* **1995**, *51*, 295–300. https://doi.org/10.5006/1.3293594.
159. Xia, D.H.; Qin, Z.; Song, S.; Macdonald, D.; Luo, J.L. Combating Marine Corrosion on Engineered Oxide Surface by Repelling, Blocking and Capturing Cl−: A Mini Review. *Corros. Commun.* **2021**, *2*, 1–7. https://doi.org/10.1016/J.CORCOM.2021.09.001.
160. Martínez-Villafañe, A.; Almeraya-Calderón, M.F.; Gaona-Tiburcio, C.; Gonzalez-Rodriguez, J.G.; Porcayo-Calderón, J. High-Temperature Degradation and Protection of Ferritic and Austenitic Steels in Steam Generators. *J. Mater. Eng. Perform.* **1997**, *7*, 108–113. https://doi.org/10.1007/S11665-006-5012-3/METRICS.
161. Pan, L.; Ding, W.; Ma, W.; Hu, J.; Pang, X.; Wang, F.; Tao, J. Galvanic Corrosion Protection and Durability of Polyaniline-Reinforced Epoxy Adhesive for Bond-Riveted Joints in AA5083/Cf/Epoxy Laminates. *Mater. Des.* **2018**, *160*, 1106–1116. https://doi.org/10.1016/J.MATDES.2018.10.034.
162. Sadek Mogoda, A.; Zohdy, K.M. Electrochemical Behavior of Titanium in NaF Solutions and Characterization of Oxide Film Formed on Its Surface. *Int. J. Electrochem. Sci.* **2020**, *15*, 8070–8085. https://doi.org/10.20964/2020.08.16.
163. Sadek, A.Z.; Zheng, H.; Latham, K.; Wlodarski, W.; Kalantar-Zadeh, K. Anodization of Ti Thin Film Deposited on ITO. *Langmuir* **2009**, *25*, 509–514. https://doi.org/10.1021/LA802456R/ASSET/IMAGES/MEDIUM/LA-2008-02456R_0001.GIF.
164. Contreras, A.; Salazar, M.; Carmona, A.; Galván-Martínez, R. Electrochemical Noise for Detection of Stress Corrosion Cracking of Low Carbon Steel Exposed to Synthetic Soil Solution. *Mater. Res.* **2017**, *20*, 1201–1210. https://doi.org/10.1590/1980-5373-MR-2016-0183.
165. Galvan-Martinez, R.; Orozco-Cruz, R.; Torres-Sanchez, R.; Martinez, E.A. Corrosion Study of the X52 Steel Immersed in Seawater with a Corrosion Inhibitor Using a Rotating Cylinder Electrode. *Mater. Corros.* **2010**, *61*, 872–876. https://doi.org/10.1002/MACO.200905441.
166. Galván-Martínez, R.; Cabrera-de la Cruz, D.; Contreras, A.; Orozco-Cruz, R. A Novel Experimental Arrangement for Corrosion Study of X60 Pipeline Steel Weldments at Turbulent Flow Conditions. *Corros. Eng. Sci. Technol*. **2016**, *51*, 400–407. https://doi.org/10.1080/1478422X.2015.1124598.
167. Jáquez-Muñoz, J.M.; Gaona-Tiburcio, C.; Chacón-Nava, J.; Cabral-Miramontes, J.; Nieves-Mendoza, D.; Maldonado-Bandala, E.M.; Delgado, A.D.; Flores-De Los Rios, J.P.; Bocchetta, P.; Almeraya-Calderón, F. Electrochemical Corrosion of Titanium and Titanium Alloys Anodized in H_2SO_4 and H_3PO_4 Solutions. *Coatings* **2022**, *12*, 325. https://doi.org/10.3390/coatings12030325.
168. Karambakhsh, A.; Afshar, A.; Ghahramani, S.; Malekinejad, P. Pure Commercial Titanium Color Anodizing and Corrosion Resistance. *J. Mater. Eng. Perform.* **2011**, *20*, 1690–1696. https://doi.org/10.1007/S11665-011-9860-0/FIGURES/9.
169. Diamanti, M.V.; Ormellese, M.; Pedeferri, M.P. Application-Wise Nanostructuring of Anodic Films on Titanium: A Review. *J. Exp. Nanosci.* **2015**, *10*, 1285–1308. https://doi.org/10.1080/17458080.2014.999261.
170. Diamanti, M.V.; Bolzoni, F.; Ormellese, M.; Pérez-Rosales, E.A.; Pedeferri, M.P. Characterisation of Titanium Oxide Films by Potentiodynamic Polarisation and Electrochemical Impedance Spectroscopy. *Corros. Eng. Sci. Technol.* **2010**, *45*, 428–434. https://doi.org/10.1179/147842208X373191.
171. Song, H.J.; Kim, M.K.; Jung, G.C.; Vang, M.S.; Park, Y.J. The Effects of Spark Anodizing Treatment of Pure Titanium Metals and Titanium Alloys on Corrosion Characteristics. *Surf. Coat. Technol.* **2007**, *201*, 8738–8745. https://doi.org/10.1016/J.SURFCOAT.2006.11.022.
172. Jeong, Y.H.; Choe, H.C.; Brantley, W.A. Corrosion Characteristics of Anodized Ti-(10-40wt%)Hf Alloys for Metallic Biomaterials Use. *J. Mater. Sci. Mater. Med.* **2011**, *22*, 41–50. https://doi.org/10.1007/S10856-010-4188-0.
173. Prando, D.; Brenna, A.; Bolzoni, F.M.; Diamanti, M.V.; Pedeferri, M.; Ormellese, M. Electrochemical Anodizing Treatment to Enhance Localized Corrosion Resistance of Pure Titanium. *J. Appl. Biomater. Funct. Mater.* **2017**, *15*, e19–e24. https://doi.org/10.5301/JABFM.5000344.
174. Prando, D.; Nicolis, D.; Pedeferri, M.P.; Ormellese, M. Pitting Corrosion on Anodized Titanium: Effect of Halides. *Mater. Corros.* **2018**, *69*, 1441–1446. https://doi.org/10.1002/MACO.201810171.
175. Wang, Z.B.; Hu, H.X.; Zheng, Y.G.; Ke, W.; Qiao, Y.X. Comparison of the Corrosion Behavior of Pure Titanium and Its Alloys in Fluoride-Containing Sulfuric Acid. *Corros. Sci.* **2016**, *103*, 50–65. https://doi.org/10.1016/J.CORSCI.2015.11.003.
176. Scully, J.C. The Electrochemical Parameters of Stress-Corrosion Cracking. *Corros. Sci.* **1968**, 8, 513–IN18. https://doi.org/10.1016/S0010-938X(68)80006-X.
177. Casillas, N.; Charlebois, S.; Smyrl, W.H.; White, H.S. Pitting Corrosion of Titanium. *J. Electrochem. Soc.* **1994**, *141*, 636–642. https://doi.org/10.1149/1.2054783/XML.
178. Nakagawa, M.; Matsuya, S.; Shiraishi, T.; Ohta, M. Effect of Fluoride Concentration and pH on Corrosion Behavior of Titanium for Dental Use. *J. Dent. Res.* **1999**, *78*, 1568–1572. https://doi.org/10.1177/00220345990780091201.
179. Ittah, R.; Amsellem, E.; Itzhak, D. Pitting Corrosion Evaluation of Titanium in NH4Br Solutions by Electrochemical Methods. *Int. J. Electrochem. Sci.* **2014**, *9*, 633–643. https://doi.org/10.1016/S1452-3981(23)07745-3.

180. Villegas-Tovar, J.; Gaona-Tiburcio, C.; Lara-Banda, M.; Maldonado-Bandala, E.; Baltazar-Zamora, M.A.; Cabral-Miramontes, J.; Nieves-Mendoza, D.; Olguin-Coca, J.; Estupiñan-Lopez, F.; Almeraya-Calderón, F. Electrochemical Corrosion Behavior of Passivated Precipitation Hardening Stainless Steels for Aerospace Applications. Metals **2023**, 13, 835. https://doi.org/10.3390/met13050835
181. Park, M.; Heo, A.; Shim, E.; Yoon, J.; Kim, H.; Joo, H. Effect of Length of Anodized TiO_2 Tubes on Photoreactivity: Photocurrent, Cr(VI) Reduction and H2 Evolution. *J. Power Sources* **2010**, *195*, 5144–5149. https://doi.org/10.1016/J.JPOWSOUR.2010.02.065.
182. Sharma, A.; McQuillan, A.J.; Sharma, L.A.; Waddell, J.N.; Shibata, Y.; Duncan, W.J. Spark Anodization of Titanium–Zirconium Alloy: Surface Characterization and Bioactivity Assessment. *J. Mater. Sci. Mater. Med.* **2015**, *26*, 221. https://doi.org/10.1007/S10856-015-5555-7/FIGURES/5.
183. Zhang, S.; Qin, J.; Yang, C.; Zhang, X.; Liu, R. Effect of Zr Addition on the Microstructure and Tribological Property of the Anodization of Ti-6Al-4V Alloy. *Surf. Coat. Technol.* **2018**, *356*, 38–48. https://doi.org/10.1016/J.SURFCOAT.2018.09.051.
184. Oliveira, N.T.C.; Guastaldi, A.C. Electrochemical Behavior of Ti–Mo Alloys Applied as Biomaterial. *Corros. Sci.* **2008**, *50*, 938–945. https://doi.org/10.1016/J.CORSCI.2007.09.009.
185. Nguyen, P.M.H.; Won, D.H.; Kim, B.S.; Jang, Y.S.; Nguyen, T.D.T.; Lee, M.H.; Bae, T.S. The Effect of Two-Step Surface Modification for Ti-Ta-Mo-Zr Alloys on Bone Regeneration: An Evaluation Using Calvarial Defect on Rat Model. *Appl. Surf. Sci.* **2018**, *442*, 630–639. https://doi.org/10.1016/J.APSUSC.2018.02.211.
186. Huang, Y.; Cai, B.; Yuan, D.; Guo, Z. Construction of Porous Micro/Nano Structures on the Surface of Ti–Mo–Zr Alloys by Anodic Oxidation for Biomedical Application. *J. Mater. Res. Technol.* **2024**, *30*, 2986–2998. https://doi.org/10.1016/J.JMRT.2024.04.046.
187. Almeraya-Calderón, F.; Jáquez-Muñoz, J.M.; Maldonado-Bandala, E.; Cabral-Miramontes, J.; Nieves-Mendoza, D.; Olgui-Coca, J.; Lopez-Leon, L.D.; Estupiñán-López, F.; Lira-Martínez, A.; Gaona Tiburcio, C. Corrosion Resistance of Titanium Alloys Anodized in Alkaline Solutions. Metals **2023**, 13, 1510. https://doi.org/10.3390/met13091510.
188. Mor, G.K.; Varghese, O.K.; Paulose, M.; Mukherjee, N.; Grimes, C.A. Fabrication of Tapered, Conical-Shaped Titania Nanotubes. *J. Mater. Res.* **2003**, *18*, 2588–2593. https://doi.org/10.1557/JMR.2003.0362/METRICS.
189. Xia, D.-H.; Song, S.; Behnamian, Y.; Hu, W.; Cheng, Y.F.; Luo, J.-L.; Huet, F. Review—Electrochemical Noise Applied in Corrosion Science: Theoretical and Mathematical Models towards Quantitative Analysis. *J. Electrochem. Soc.* **2020**, *167*, 081507. https://doi.org/10.1149/1945-7111/AB8DE3.
190. Casanova, L.; La Padula, M.; Pedeferri, M.P.; Diamanti, M.V.; Ormellese, M. An Insight into the Evolution of Corrosion Resistant Coatings on Titanium during Bipolar Plasma Electrolytic Oxidation in Sulfuric Acid. *Electrochim. Acta* **2021**, *379*, 138190. https://doi.org/10.1016/J.ELECTACTA.2021.138190.
191. Fekry, A.M. The Influence of Chloride and Sulphate Ions on the Corrosion Behavior of Ti and Ti-6Al-4V Alloy in Oxalic Acid. *Electrochim. Acta* **2009**, *54*, 3480–3489. https://doi.org/10.1016/J.ELECTACTA.2008.12.060.
192. Puga, M.L.; Venturini, J.; ten Caten, C.S.; Bergmann, C.P. Influencing Parameters in the Electrochemical Anodization of TiO_2 Nanotubes: Systematic Review and Meta-Analysis. *Ceram. Int.* **2022**, *48*, 19513–19526. https://doi.org/10.1016/J.CERAMINT.2022.04.059.
193. Degirmenci, K.; Saridag, S. Influence of Anodized Titanium Abutment Backgrounds on the Color Parameters of Different Zirconia Materials. *Am. J. Dent.* **2021**, *34*, 39–43.
194. Lara-Banda, M.; Gaona-Tiburcio, C.; Zambrano-Robledo, P.; Delgado-E.M.; Cabral-Miramontes, J.A.; Nieves-Mendoza, D.; Maldonado-Bandala, E.; Estupiñan-López, F.; Chacón-Nava, J.G.; Almeraya-Calderón, F. Alternative to Nitric Acid Passivation of 15-5 and 17-4PH Stainless Steel Using Electrochemical Techniques. Materials **2020**, 13, 2836, doi:10.3390/ma13122836.
195. Hernández-López, J.M.; Conde, A.; de Damborenea, J.; Arenas, M.A. Correlation of the Nanostructure of the Anodic Layers Fabricated on Ti13Nb13Zr with the Electrochemical Impedance Response. *Corros. Sci.* **2015**, *94*, 61–69. https://doi.org/10.1016/J.CORSCI.2015.01.041.
196. Shukla, A.K.; Balasubramaniam, R. Effect of Surface Treatment on Electrochemical Behavior of CP Ti, Ti–6Al–4V and Ti–13Nb–13Zr Alloys in Simulated Human Body Fluid. *Corros. Sci.* **2006**, *48*, 1696–1720. https://doi.org/10.1016/J.CORSCI.2005.06.003.
197. Choi, Y.; Jeong, C. Influence of Electrolyte on the Shape and Characteristics of TiO_2 during Anodic Oxidation of Titanium. *Corros. Sci. Technol.* **2023**, *22*, 193–200. https://doi.org/10.14773/CST.2023.22.3.193.
198. Suhadolnik, L.; Marinko, Ž.; Ponikvar-Svet, M.; Tavčar, G.; Kovač, J.; Čeh, M. Influence of Anodization-Electrolyte Aging on the Photocatalytic Activity of TiO_2 Nanotube Arrays. *J. Phys. Chem. C* **2020**, *124*, 4073–4080. https://doi.org/10.1021/ACS.JPCC.9B09522/SUPPL_FILE/JP9B09522_SI_001.PDF.
199. Ohtsu, N.; Komiya, S.; Kodama, K. Effect of Electrolytes on Anodic Oxidation of Titanium for Fabricating Titanium Dioxide Photocatalyst. *Thin Solid Film* **2013**, *534*, 70–75. https://doi.org/10.1016/J.TSF.2013.01.106.
200. Choi, Y.; Jeong, C. Investigating the Influence of Pore-Widening Time Control in Electrochemical Anodization for the Formation of Hybrid Titanium Nanostructures with Enhanced Superhydrophobicity for Improved Corrosion Resistance Efficiency. *Electrochim. Acta* **2024**, *492*, 144380. https://doi.org/10.1016/J.ELECTACTA.2024.144380.
201. Bouchama, L.; Bouznit, Y.; Boukmouche, N.; Irki, S. Two-Step vs. Single-Step Electrochemical Anodizing Process Regarding Anti-Corrosion Properties of Titanium. *Anal. Bioanal. Electrochem.* **2023**, *15*, 264–279. https://doi.org/10.22034/abec.2023.704566.
202. Winiarski, J.; Niciejewska, A.; Górnik, M.; Jakubowski, J.; Tylus, W.; Szczygieł, B. Titanium Anodizing in a Choline Dihydrogencitrate Salt–Oxalic Acid Deep Eutectic Solvent: A Step towards Green Chemistry in Surface Finishing of Titanium and Its Alloys. *RSC Adv.* **2021**, *11*, 21104–21115. https://doi.org/10.1039/D1RA01655E.

203. Lazarouk, S.K.; Sasinovich, D.A.; Kupreeva, O.V.; Orehovskaia, T.I.; Rochdi, N.; D'Avitaya, F.A.; Borisenko, V.E. Effect of the Electrolyte Temperature on the Formation and Structure of Porous Anodic Titania Film. *Thin Solid Film.* **2012**, *526*, 41–46. https://doi.org/10.1016/J.TSF.2012.10.112.
204. Pokrowiecki, R.; Mielczarek, A.; Zaręba, T.; Tyski, S. Oral Microbiome and Peri-Implant Diseases: Where Are We Now? *Ther. Clin. Risk Manag.* **2017**, *13*, 1529. https://doi.org/10.2147/TCRM.S139795.
205. Zhang, Y.; Zheng, X.; Wang, N.; Lai, W.H.; Liu, Y.; Chou, S.L.; Liu, H.K.; Dou, S.X.; Wang, Y.X. Anode Optimization Strategies for Aqueous Zinc-Ion Batteries. *Chem. Sci.* **2022**, *13*, 14246–14263. https://doi.org/10.1039/D2SC04945G.